Enhacement of Microgrid Technologies using Various Algorithms

Saleh Masoud Abdallah Altbawi[a], Dr. Ahmad Safawi Bin Mokhtar[b], and Zeeshan Ahmad Arfeen[c]

[a]
Electrical Engineering department, University Technology Malaysia
Qollege of Sciences and Technology Umalaranib, Libya
[b]Senior Lecturer, School of Electrical Engineering
Universiti Teknologi Malaysia, Johor Bahru, Johor, Malaysia
[c]Electrical Engineering department, School of Electrical Engineering, Universiti
Teknologi Malaysia, 81310 Skudai, Johor Bahru, Johor- Malaysia.

Article History: Received: 10 January 2021; Revised: 12 February 2021; Accepted: 27 March 2021; Published online: 16 April 2021

Abstract: The electric power systems around the globe are gradually shifting from conventional fossil fuel-based generating units to green renewable energy sources. The motivation behind this change is the environmental and economic concerns. Furthermore, the existing power systems are being overloaded day by day due to the continuously increasing population, which consequently led to the overloading of transformers, transmission, and distribution lines. Despite the overwhelming advantages of renewable energy sources, there are few major issues associated with them. For example, the injection and detachment of DGs into the current power system causes disparity among produced power along with connected load, thus distracting system's equilibrium and causes unwanted voltage and frequency oscillations and overshoots. These oscillations and overshoots may cause the failure of connected equipment or power system if not properly controlled. The investigation as such challenges to improve the frequency and voltage, the islanded's power regulation and connected MG under source and load changes, which contain classic and artificial intelligence techniques. Moreover, these techniques are used also for economic analysis. To evaluate the exhibitions of microgrid (MG) operations and sizing economic analysis acts as a significant tool. Optimization method is obligatory for sizing and operating an MG as reasonably as feasible. Diverse optimization advances remain pertained to microgrid to get optimal power flow and management.

1. Introduction

Microgrid is said to be the distributed generation (DG) units' agglomeration generally related via power automatic based system to effectiveness grid. Non-conservative energy supplies like fuel cells, hydroelectric power, wind turbines as well as solar power are used to prepare DG Units. Microgrid could work by attached towards grid or segregated from grid. Difficulties of power quality impact is concerning whilst connecting microgrid and main grid whereas it can turn out to be a primary part for exploration. If voltage unbalance is troubling, the solid state circuit breaker (CB) allied to the MG along with effectiveness grid will release to segregate the microgrid. While unbalance in voltage weak, CB stay clogged, ensuing in continued disturb voltage at the time of mutual coupling. Normally quality of power issue is older in electric system, except improvement of methodology expanded lately[1].

1.1 Reference Frames of space vectors

Fixed frame abc

Also called symmetrical components which are electrical system of generic three-phase that consists of a cluster of three voltages along with three currents interrelating among one another for electrical power delivering. The steady-state current three-phase waveforms unstable scheme in the company of phasor portrayal taking place in Gauss plane [2].

$$V_a = V_{LN}\angle 0^{\circ} \quad (1)$$

$$V_b = V_{LN}\angle -120^{\circ} \quad (2)$$

$$V_c = V_{LN}\angle +120^{\circ} \quad (3)$$

These voltages feed into either a Wye(Y) or Delta connection.

The voltage observed by the load will rely on the load connection, for the wye case linking every phase (line to neural) voltages will give these currents[3]:

$$i_a = \frac{V_a}{|Z_{total}|}\angle -\theta^0 \quad (4)$$

$$i_b = \frac{V_b}{|Z_{total}|}\angle (-120-\theta)^0 \quad (5)$$

$$i_c = \frac{V_c}{|Z_{total}|}\angle(120-\theta)^0 \quad (6)$$

Where Z_{total} is the summation of line and load impedances ($Z_{total} = Z_{LN} + Z_Y$), and θ is the phase of the total impedance (Z_{total}). The phase angle involving voltage and current of each phase depends on the type of Z_Y inductive and capacitive loads which cause current to either delay or guide the voltage but resistance equal to zero. Nevertheless, the relative phase among each pair of lines will be -120^0.

Let, i_a, $i_b$and i_c be immediate steady three-phase currents. Next,

$$i_a + i_b + i_c = i_N = 0 \quad (7)$$

Present space vector is signified in the name of phase currents as

$$\bar{\imath} = k\,(i_a + a\,i_b + a^2 i_c) \quad (8)$$

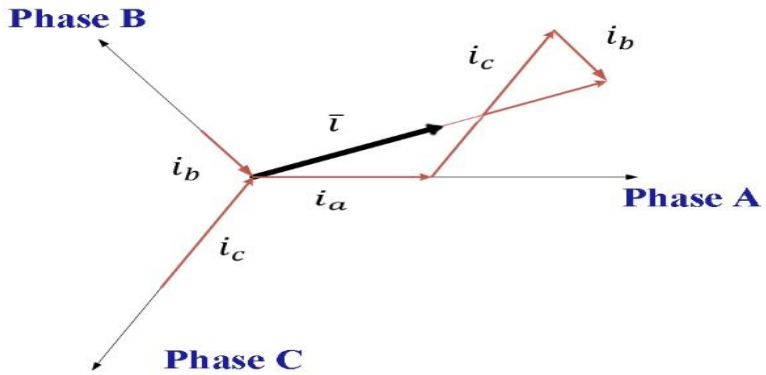

Figure (1) Present space vector along with the protuberance

Here, 'a' is operator depicted previously, also 'k' is Transformation constant.

Figure 1 illustrates the space current vector with the protuberance [4].

General Rotating Reference Frame

Moreover, frame of stationary reference is affixed with stator; equations of present space vector are devised in a common reference frame that revolved in common speed ω_G as exposed by Figure (2).

If common reference frames are employed through direct and quadrature axes (x and y) revolving in common immediate swiftness,$\omega_G = d\theta_G/dt$, exposed by Fig 2, whereas $\theta_G$is angle amid stationary reference frame's (α) direct axis connected to real axis (x) of common orientation frame and present space vector in common orientation frame could be inscribed by

$$\bar{\imath}_G = \bar{\imath}e^{-j\theta G} = (i_x + i_y)[2]. \quad (9)$$

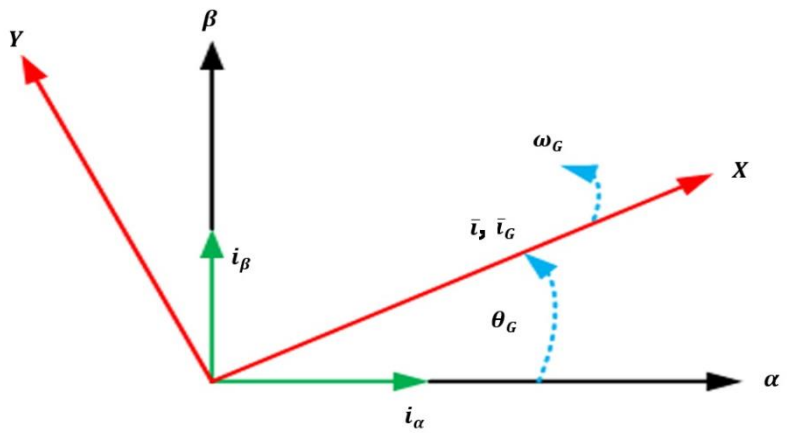

Figure (2) General rotating frame of reference

Stationary Reference Frame

Space vector is able to be conveyed using two-axis theory. Actual piece of space vector is equivalent to instant significance of current component's direct-axis (i_α), with imaginary part being equivalent to current component's quadrature-axis (i_β).

Hence, the present space vector within the inactive reference frame can be stated as:

$$\bar{\imath} = (i_\alpha + i_\beta)$$

In balanced 3-phase technologies, the quadrature and currents of direct axis i_α and i_β remain current components of fabricated quadrature-phase, that is associated towards definite 3-phase currents[5]. like:

$$i_\alpha = k\left(i_a - \frac{1}{2}i_b - \frac{1}{2}i_c\right) \qquad (10)$$

$$i_\beta = k\frac{\sqrt{3}}{2}(i_a - i_b) \qquad (11)$$

$$\begin{bmatrix} v_\alpha \\ v_\beta \\ v_0 \end{bmatrix} = \frac{2}{3}\begin{bmatrix} 1 & -\frac{1}{2} & -\frac{1}{2} \\ 0 & \frac{\sqrt{3}}{2} & -\frac{\sqrt{3}}{2} \\ \frac{1}{\sqrt{2}} & \frac{1}{\sqrt{2}} & \frac{1}{\sqrt{2}} \end{bmatrix}\begin{bmatrix} v_a \\ v_b \\ v_c \end{bmatrix}$$

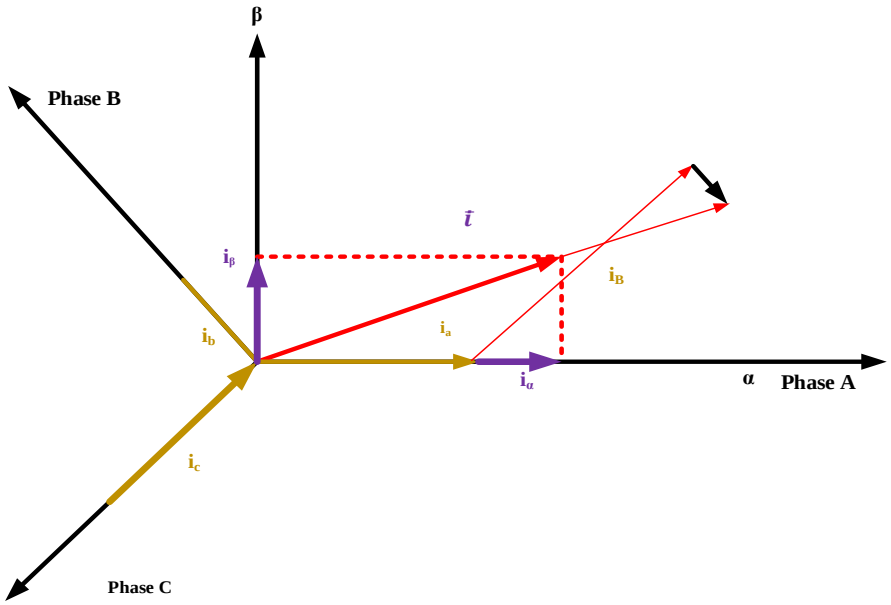

Figure (3) Present space vector (α, β) plane

d-q Rotating Reference Frame

The coordinated orientation frame, otherwise called dq reference frame depends on two symmetrical dq axes, revolving at frequencyω,that is set at $\theta = \omega\, t$ precise point on $\alpha\beta$ plane. Gratitude to its revolving quality where revolution is extensively employed in study of electrical equipment's. The transformation matrix for interpreting a voltage vector since $\alpha\beta 0$ stationary reference border to $dq0$ coordinated reference border is specified as

$$\begin{bmatrix} v_d \\ v_q \\ v_0 \end{bmatrix} = \frac{2}{3}\begin{bmatrix} \cos(\theta) & \sin(\theta) & 0 \\ -\sin(\theta) & \cos(\theta) & 0 \\ 0 & 0 & 1 \end{bmatrix}\begin{bmatrix} v_\alpha \\ v_\beta \\ v_0 \end{bmatrix}$$

Thus, transformation matrix to decode a voltage vector starting abc stationary reference frame to $dq0$ coordinated reference border is agreed as [4]:

$$\begin{bmatrix} v_d \\ v_q \\ v_0 \end{bmatrix} = \sqrt{\frac{2}{3}} \begin{bmatrix} \cos(\theta) & \cos(\theta - \frac{2\pi}{3}) & \cos(\theta + \frac{2\pi}{3}) \\ -\sin(\theta) & -\sin(\theta - \frac{2\pi}{3}) & -\sin(\theta + \frac{2\pi}{3}) \\ \frac{1}{\sqrt{2}} & \frac{1}{\sqrt{2}} & \frac{1}{\sqrt{2}} \end{bmatrix} \begin{bmatrix} v_a \\ v_b \\ v_c \end{bmatrix}$$

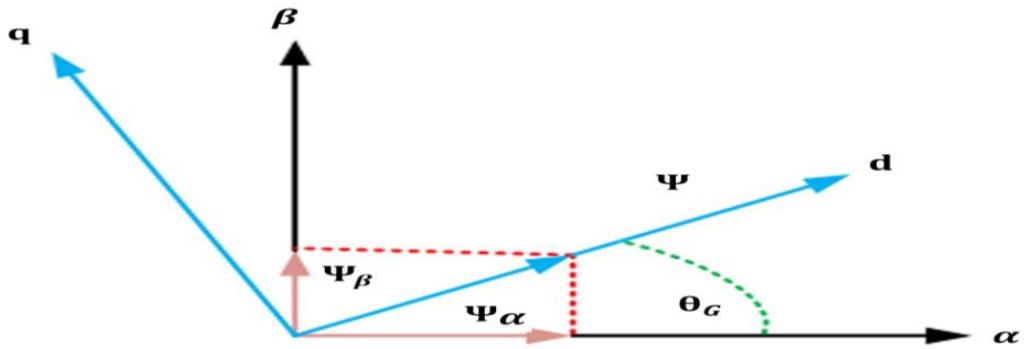

Figure (4) d-q rotating frame of reference

Transformation Matrices

The transformations illustrated within preceding segments could be abridged in common outline by,

$$\begin{bmatrix} \alpha \\ \beta \end{bmatrix} = [Clarke\ Matrix] \times \begin{bmatrix} a \\ b \\ c \end{bmatrix} \quad (12)$$

$$\begin{bmatrix} d \\ q \end{bmatrix} = [Park\ Matrix] \times \begin{bmatrix} \alpha \\ \beta \end{bmatrix} \quad (13)$$

$$\begin{bmatrix} d \\ q \end{bmatrix} = [Park\ Matrix] \times [Clarke\ Matrix] \times \begin{bmatrix} a \\ b \\ c \end{bmatrix} \quad (14)$$

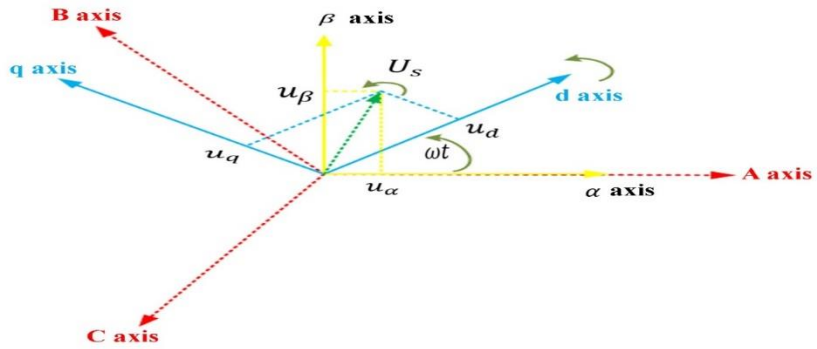

Figure (5) (a-b-c), (d-q) and (α-β) reference frames

The transformation between abc, Park plane and Clarke plane is revealed by illustrated in Fig. 5. For both phase currents and phase voltages, these transformations can be applied.

The p-q theory is so great that it has been as of now applied to the regulator circuit of reactive power compensators and active power filters utilizing exchanging gadgets like GTO thyristors and IGBT[2].

The PWM controller investigation is apprehended for d-q and α-β reference frames. PWM regulator exercising α-β orientation frame is much proficient along with steady-state offers lesser harmonic constituents in the voltages of load in addition to source currents [6].

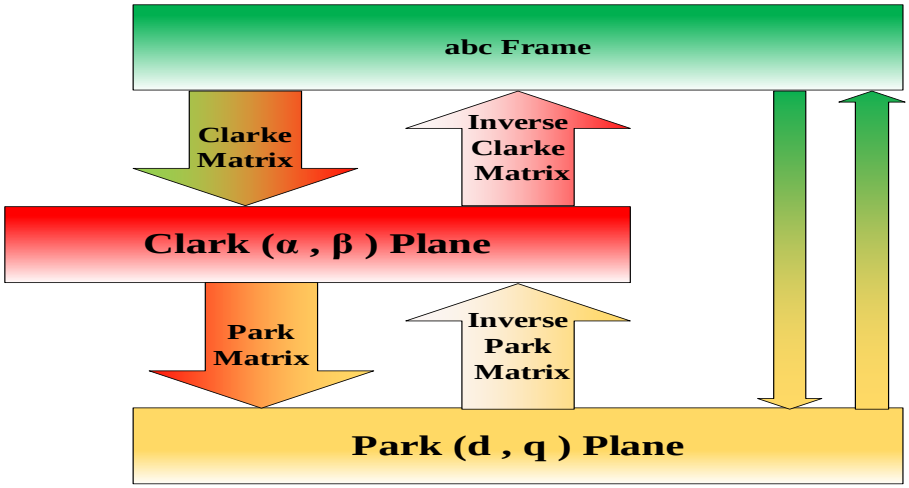

Figure (6) Transformation of reference frame

COMPENSATORS IN MICROGRID FOR POWER QUALITY ENHANCEMENT

Here[7][8], compensators utilization decline of harmonics in a dispersed microgrid is emphasized by various authors. In [9], the area of harmonic current sharing used a load compensator. Examining grid-side inductances' difficulties of the compensator is planned in the company of impedance loops: variable harmonic impedance (VHI) loop, virtual fundamental impedance (VFI) loop. The droop controller of reactive power-voltage (Q-V) and active power-frequency (P-ω) presentations were sustained by VFI loop. By introducing VFI[10] the negative cycle circulating current is also lessened in this compensator. It [11] associations voltage inertia and virtual impedance to improve Virtual synchronous generator control. This method reduces power originated by the power instabilities. It efficiently lessen the influence of sound of high frequency on the voltage. In [12], a new checking controller for sub-synchronous resonance (SSR) alleviation exercising current variable frequency created on an Auxiliary Damping Controller (ADC). This strategy is effective in offering constructive damping to alleviate unbalanced SSR oscillations beneath a variety of functioning circumstances. Paper [13] used an switched filter compensator, distribution synchronous inert compensator and PID controller tuned by means of GOA. These scenarios are used separately and produced acceptable performance with alleviation of harmonics deformation, decrease of devoured reactive power and power factor. Moreover, these methods are self-tuned more effective.

POWER QUALITY IMPROVEMENT WITH CONTROLLERS

The control strategy for balancing the unbalance voltage in different operating condition in microgrid is argued in this part. The method at hand in [14][15][16] worked to reduce voltage unbalance in common coupling (PCC) moment. The issue inside document is characterized as voltage disturbance remuneration on PCC along with voltage quality improvement by Sensitive Load Bus (SLB). Here, at difficult plan, the use of the progressive control strategy that encompasses most important and less important control levels was offered. Into [14], impedance power fall reparation is supplementary to enhanced droop control for normalizing no-load power amplitude for guaranteeing production power is regular. In[15], added part to the controller with the aspiration for enhancement of the voltage unbalance factor (VUF) equivalent at all sensitive load bus(SLB) which that produces far superior outcomes for swiftness along with exactness of managing goals. In[16], the paper includes Z-Q droop control as the Traditional power distribution strategies contain nil impact with Q by pessimistic progression present data. By utilizing the droop control along with the traditional droop control algorithm, a whole power distribution system is put forward.

ROLE OF APC IN POWER QUALITY IMPROVEMENT

Diverse crisis analysis is ventured through Vechiu et al. [17] and Balanuta et al. [18] and improvement of power and current factor as the center boundaries [17] is seen. The interface of AC bus in the company of environment friendly power supplies by active power conditioner (APC) in microgrid. Consequently, in favour of the power excellence upgradation, APC should be managed. In [17], an innovative controller stratagem amid PI controllers along with hysteresis controller is ventured. The ventured controller plan utilizes reparation system which compels current after microgrid for getting adjusted and sinusoidal by formulating the APC recompense load current. A new control strategy assists in permitting power by infused in microgrid, recompensing current harmonics, correcting power factor along with stabilizing supply voltage of PCC. Limitation of employing hysteresis control is altering changing rate that produces group of important side harmonics in the area of changing rate. Control policy logic is ensured by Matlab simulation software [17]. Vechiu et al. has completed the contextual analysis where coming up is the derivations.

(i) Reparation of harmonics: the established control methodology decreased microgrid's THD current near 3%, likewise permitted microgrid current remaining constant.

(2) Rectification of power factor: the power factor amid electricity as of microgrid along with supply of voltage is constructed unison by assistance of APC controller methodology.

(3) Unstable load: a resistive type three-phase load persuades unstability in method, that's remunerated with APC.

By APC control, level of unstability is fewer than 0.8% that's under allowed stage of 2% of global principles [1].

PHASE GRID-CONNECTED VOLTAGE SOURCE INVERTER SYSTEM MODELING:

Framework of 3-phase associated by Voltage Source Inverter structure through LC filter. At this point, 'Ls, Rs' are same bumped inductance just like filter's resistance, if relevant coupling transformer, just like the grid seen by inverter. Filter capacitance is 'C', grid voltage is 'Vs'. Insulated Gate Bipolar Transistor kind DC-AC converter is thought of. State-space equation of the design for the reference frame "abc" is specified underneath:

$$\frac{d}{dt}\begin{bmatrix} i_a \\ i_b \\ i_c \end{bmatrix} = \frac{R_s}{L_s}\begin{bmatrix} i_a \\ i_b \\ i_c \end{bmatrix} + \frac{1}{L_s}\left(\begin{bmatrix} V_{sa} \\ V_{sb} \\ V_{sc} \end{bmatrix} - \begin{bmatrix} V_a \\ V_b \\ V_c \end{bmatrix}\right) \quad (15)$$

The equation is conveyed through Using Park's transformation as

$$\frac{d}{dt}\begin{bmatrix} i_d \\ i_q \end{bmatrix} = \begin{bmatrix} -\frac{R_s}{L_s} & \omega \\ -\omega & -\frac{R_s}{L_s} \end{bmatrix} + \frac{1}{L_s}\left(\begin{bmatrix} V_{sd} \\ V_{sq} \end{bmatrix} - \begin{bmatrix} V_d \\ V_q \end{bmatrix}\right) \quad (16)$$

$i_{dq0} = \tau\, i_{abc}$ where;

$i_{dq0} = \begin{bmatrix} i_d \\ i_q \\ i_0 \end{bmatrix}$; $i_{abc} = \begin{bmatrix} i_a \\ i_b \\ i_c \end{bmatrix}$ and transformation τ is

$$\tau = \sqrt{\frac{2}{3}}\begin{bmatrix} \cos(\theta) & \cos(\theta - \frac{2\pi}{3}) & \cos(\theta + \frac{2\pi}{3}) \\ -\sin(\theta) & -\sin(\theta - \frac{2\pi}{3}) & -\sin(\theta + \frac{2\pi}{3}) \\ \frac{1}{\sqrt{2}} & \frac{1}{\sqrt{2}} & \frac{1}{\sqrt{2}} \end{bmatrix} \quad (17)$$

where'T', 'ω' is transformation matrix and angular frequency [19].

Voltage Source Inverter (VSI)

Inverters are static power converters that create AC production wave structure as of DC power contribution. If a DC input is a voltage resource, in that case the inverter is known as a Voltage Source Inverter (VSI). The VSI route has an ability of managing AC output voltage, whereas CSI straightly manages AC output current. As per various phases, inverters are categorized into two types:

- Single-phase half-bridge inverter
- Single-phase full-bridge inverter
- Three-phase voltage source inverter[20]

For three-stage three level inverter design alike, utilized by 12 electronic devices (IGBT) are necessary. Every point exchanges through three voltage stages (+$V_{dc/2}$, 0, -$V_{dc/2}$). Within three-phase two-level inverter Pulse Width Modulation age algorithms generates least harmonic distortion. A lot of researchers utilized three-level inverter for the reason that the intrinsic unbiased-point probable disparity of a three-level inverter is successfully concealed for completely using the previously declared benefits of three-level inverter. Numerous PWM methods are offered for resolving neutral- point probable unstable issue [21].

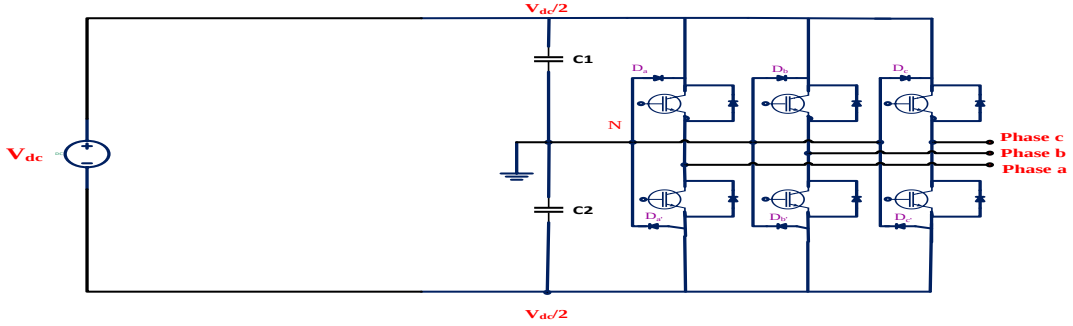

Figure (7) Route illustration of two-level inverter

Insulated-gate Bipolar Transistor (IGBT)

The Insulated Gate Bipolar Transistor called as IGBT, is a cross amid a regular Bipolar Junction Transistor, (BJT) along with Field Effect Transistor, (MOSFET) formulating as supreme like semiconductor exchanging gadget.

The IGBT Transistor obtains most amazing aspects of two kinds of basic transistors, the elevated input impedance along with elevated exchanging rates of MOSFET through short diffusion voltage of bipolar transistor, uniting jointly to make an extra sort of transistor exchanging gadget, proficient for managing huge collector-emitter currents by nearly zero gate current drive [22].

IGBT contain exchanging features sesame as MOSFET, with elevated current addition to voltage limits of bipolar junction transistor (BJT) [3]. Production of IGBT is akin to perpendicular dispersion power MOSFET, apart from extra film over collector as shown in Fig. 1. The focal feature of perpendicular preparation is collector (drain) organizes device's lower part whereas emitter (source) area remains as before like regular MOSFET. Figure 1 tends to designed plan of gadget utilized in process. The additional film of IGBT proceeds like foundation of holes which are implanted towards the body (n- region) through the process. The implanted holes allow speedy turn-off by recombination of surplus electrons which stay in body of IGBT behind switch-off [23].

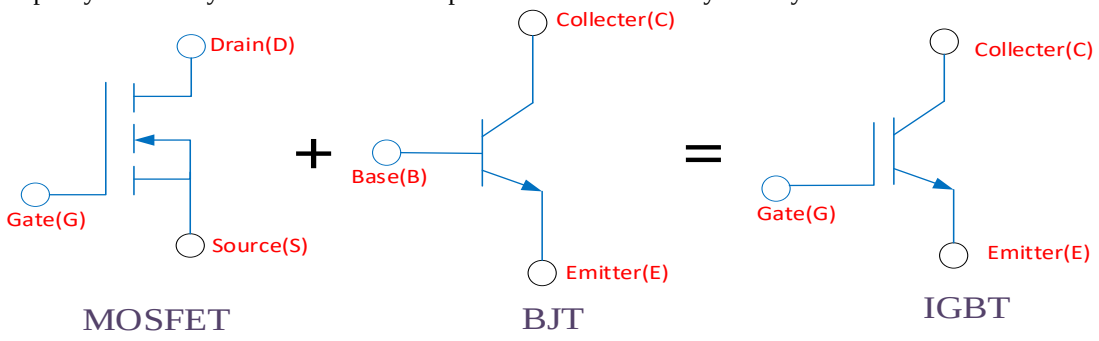

Figure (8) MOSFET, BJT and IGBT

Low Pass Filter

A low-pass filter (LPF) surpasses indications by a frequency lesser to chosen cut off frequency, also deteriorates indications with frequencies elevated than cut off frequency. Accurate frequency reaction of filter relies on filter design. Filter at times is known a high-cut filter, otherwise treble-cut filter at acoustic functions. It is using in microgrid to overpower harmonics and spurious is a mutual system in manipulative a power amplifier, voltage-controlled oscillator and mixer [24].

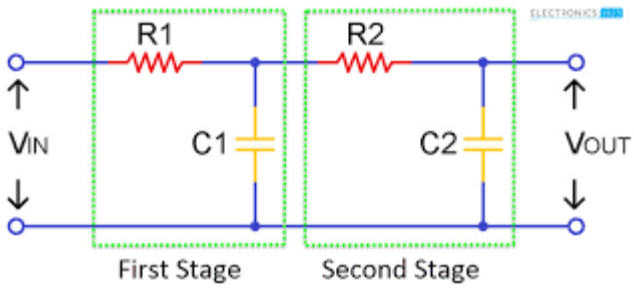

Figure (9) second order low pass filter

Transmit role of second-order low-pass filter is specified:

$$T(s) = \frac{a_0}{s^2+(\omega_p/Q)s+\omega_p{}^2,} \qquad (18)$$

Where a_0, ω_p and Q, the limitations of filter, $s = i\omega,$ in the company of $i = \sqrt{-1}$ as well as ω, angular rate of recurrence of relevant sine wave.

Increase of secondary-order low pass filter is only the enormity of eq (18)

And can put in writing like equation (below)

$$|T(\omega)| = \frac{|a_0|}{\sqrt{\left(\omega_p{}^2/\omega^2\right)^2+(\omega p\omega/Q)^2}} \qquad (19)$$

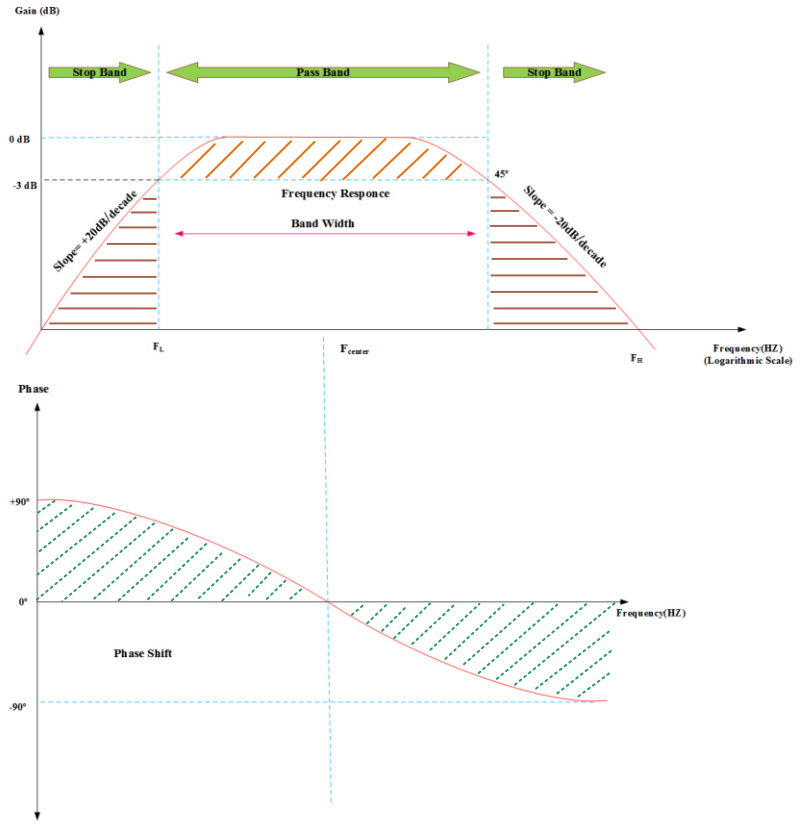

Figure (10) low pass filter wave form

Pulse Width Modulation (PWM)

PWM controller, accountable for guaranteeing the right amalgamation of these signs is via compensators. Like robusteras the PWM controller is, enhanced presentation, thus permitting circuitous turbulence alleviation offered [16]. At the end of the day, as model, if the sequence compensators are a proficient current supply, the impedance of harmonic load currents is elevated. Subsequently, single trail for flows is drained by shunt compensator, the low impedance voltage source. Similar investigation is prepared for voltage supply turbulences. For model, when droop voltage happens in supply bus, that doesn't have an effect on the load bus, as the shunt compensator is a productive voltage source associated at the load bus. Subsequently, the recompensation voltage in the sequence compensator workstation [7]. By and large, incessant PWM (CPWM) along with Discontinuous PWM (DPWM) are different kinds of PWM. Continuous PWM is one of the PWM kinds as it has constant signal all through the balancing indication phase. Discontinuous PWM is another sort that is deliberately placed equivalent to summit transporter indication where exchanging doesn't happen to the slightest 40% transporter indication phase [25]. Hysteresis pulse width modulation, Selective Harmonic Elimination pulse width modulation (SHEPWM), third harmonic injection pulse width modulation (THIPWM). Hysteresis regulator is utilized for source inverter Current and residual PWM methods were employed for source inverter Voltage. Space Vector pulse width modulation (SVPWM) and Sinusoidal Pulse width modulation (SPWM) techniques are much broadly utilized. They control the output voltage and decrease the harmonics.

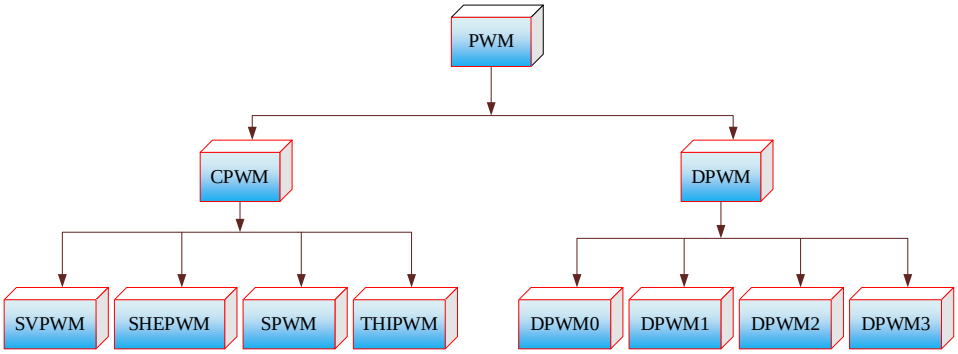

Figure (11) Types of PWM

The fundamental guideline of the proposed SVPWM strategy can be effortlessly clarified. The three-level inverter space-vector chart revealed in Figure(11) could be felt it's created of six little hexagons which being space-vector diagrams of conventional two-level inverters. Every six hexagons, comprising space-vector illustration of three-level inverter, centers on six apexes of internal little hexagon like is exposed by Figure (12) [21][26].

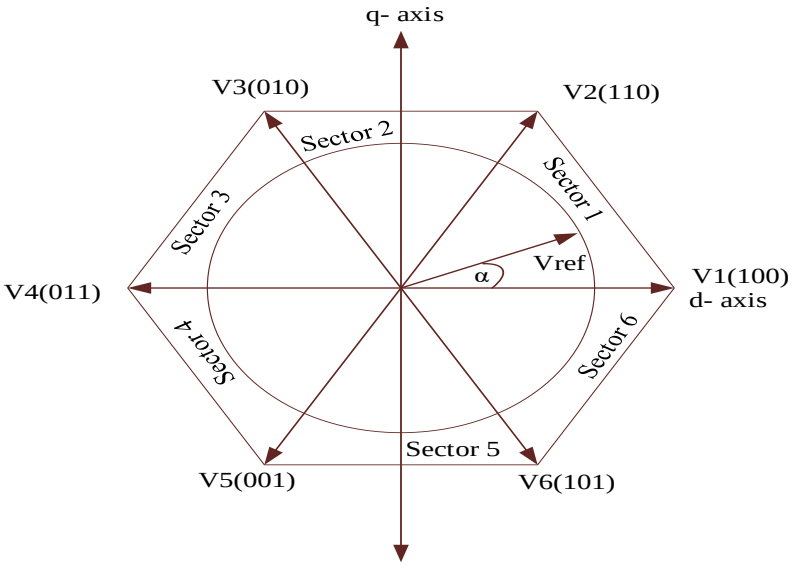

Figure (13) Vector Representation of SVPWM Signal

When the value is resoluted, the root of voltage vector's reference is transformed to middle voltage vector of chosen hexagon. It's finished through deducting middle vector of chosen hexagon since first reference vector, like demonstrated by Figure (14) [21].

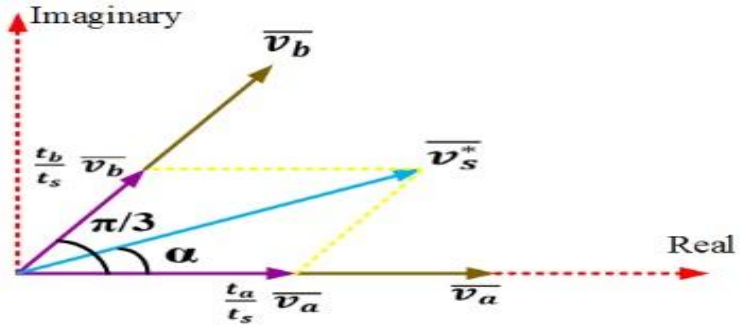

Figure (14) highest accessible basic output voltage of PWM

Accordingly, highest accessible basic output voltage:

$$|\overrightarrow{v_s^*}| = \frac{2}{3}V_{dc}\left(\frac{\pi}{6}\right) = \frac{1}{\sqrt{3}}V_{dc} \quad (20)$$

The reference vector that addresses three-phase sinusoidal voltage is produced by SVPWM through exchanging among the two closest active vectors as well as zero vectors. For ascertaining hour of utilization for diverse vectors, think Fig. 4, portraying situation distinctively accessible space vectors as well as reference vector of first sector [27]. Because of utilizing Pulse Width Modulation (PWM) of inverters, that contain nonlinear voltage-current qualities while exercising semiconductor parts as well as could generate elevated exchanging rate of recurrence - with satisfactory vibrant reactions, an insufficient total harmonic distortion (THD) resulting as that doesn't generate zero voltage vectors. To conquer the cons of PWM by relating numerous techniques and to tackle intricate nonlinear equations is to discover the finest switching timing. The computation process comprise newton-rapshon, Fourier transform as well as bio-inspired algorithm approach like ant, bat, bee, particle swarm, genetic etc [28].

PI / PD/ PID controller

In the company of a shaft at the origin along with another in perpetuity, the PID controller might be believed a great form of a phase lead-lag compensator. Likewise, the cousins, PI as well as PD controllers, could be observed like extraordinary types of phase-lag as well as phase-lead compensators, correspondingly. A regular PID controller is usually called as "three-term" controller, whose transport purposes are usually written by "parallel form" specified through (1) else "ideal form" specified through

$$G(t) = K_P e(t) + K_I \int_0^t e(t) + K_D \frac{d\,e(t)}{dt}$$

$$G(s) = K_P + K_I \frac{1}{s} + K_D s$$

$$= K_P\left(1 + \frac{1}{T_I s} + T_D s\right) \quad (21)$$

here is K_P - proportional gain, K_I - integral gain, K_D - derivative gain, T_I - integral time constant, T_D - derivative time constant [29].

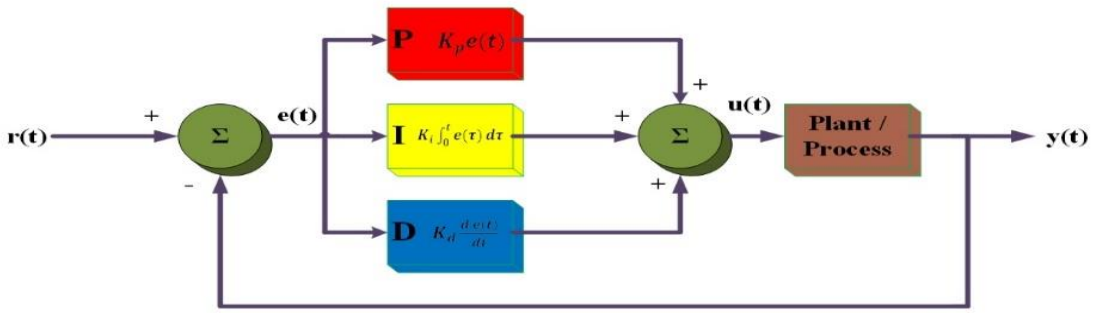

Figure (15) PID Controller

For ages, due to their basic arrangement, PI/PID controller used broadly in industrialized field as well as power scheme. PID/PI is tough, dependable as well as supplies near-optimal presentation of control method by suitable amendment increase. Quite a lot of schemes initiated to regulate the PID gains specifically, Ziegler and Nichols, Cohen Coon, Chien, Hrones and Reswick method (CHR), fine tuned as well as law of thumb [71–73]. Conversely, major drawback of PI/PID controllers is their capacity of ideally amending PID gain for nonlinear as well as composite methods. Inside framework, PID performance considerably depends on sufficient estimations of PID boundaries. For defeating the problem, a self-tuning PI/PID regulator is effectively expanded for choosing best estimation of PID coefficients [30][31].

Fuzzy logic controller

Fuzzy set theory as well as fuzzy logic sets up regulations of nonlinear mapping [9]. Utilization for fuzzy sets gives foundation of an organized means to relevance of tentative as well as imprecise representations [10]. Fuzzy control depends on rational method known fuzzy logic, lot nearer by soul in the direction of human reasoning as well as innate lingo than old style rational methods [11]. These days fuzzy logic is employed at practicall every areas of business as well as science. One is load-frequency control [7]. Fundamental objective of load-frequency control at interrelated power methods is for securing equilibrium among construction as well as expenditure [32].

The theory of fuzzy decree depends at variables of input such as error E and error variation ΔE along with output variable ΔD. The production value of variable makes DC/DC converter for discovering MPPT is resolute

by fact table by altering input limits. Major fuzzy logic controller FLC comprises three phases: fuzzification, inference and defuzzification.

Reason for fuzzification is for changing input variables to fuzzy variables. Fault E (k) as well fault variation ΔE (k) at the moment k that is described:

$$\mathrm{E(k)} = \frac{\mathrm{P(k)} - \mathrm{P(k-1)}}{V(k) - V(k-1)}$$

Then $\Delta E(k) = \mathrm{E(k)} - \mathrm{E(k-1)}$ (22)

Negative Big (NB), Negative Small (NS), Zero (ZE), Positive Big (PB) and Positive Small (PS) will be eligible by the linguistic variables.

Inference is a stage which comprises of characterizing a rational connection amid the contribution as well production as per function of system management.

Defuzzification is a method employed for changing linguistic fuzzy to definite as well important assessment.

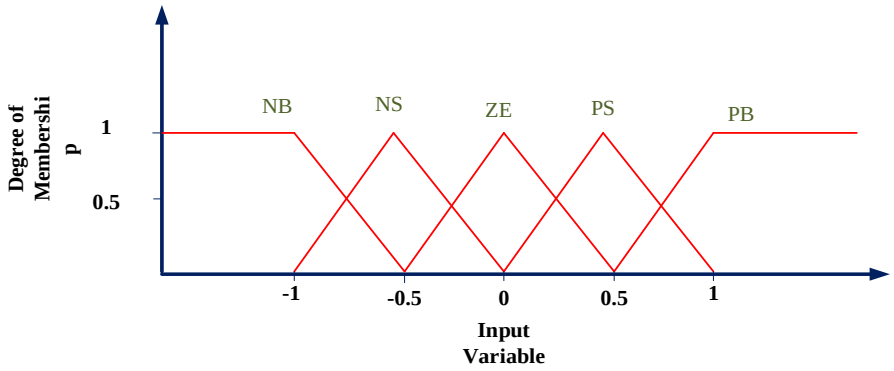

Table1 portrays the standard table of projected fuzzy logic controller enhanced through Boukezata in [14], input variables are ΔP and ΔV as well ΔD (duty cycle) is output signal that produces switching indication of boost converter is contrasted with the transporter signal [33][31][34].

Table (1) Rule Table

ΔE / E	NB	NS	ZE	PS	PB
NB	PS	PB	PB	NB	NS
NS	ZE	PS	PS	NS	ZE
ZE	ZE	ZE	ZE	ZE	ZE
PS	ZE	NS	NS	PS	ZE
PB	ZS	NB	NB	PB	PS

Phase-Locked-Loop (PLL)

Phase locked loop (PLL) is a primary model P widely utilized for diverse functions in different areas of electrical engineering e.g. interactions, instrumentation, control system, and multimedia machinery [l]. The foremost thought of phase-locking is the skill to produce a sinusoidal signal, whose stage is comprehensibly pursing input signal's central constituent [2], [3]. For quite a few years, PLLs have been the topic of R&D [5], [6]. The considerable latest progress in microelectronics faced remarkable effect on the PLL innovation. The block illustration of PLL is portrayed through Figure 1. Stage contrast among input as well output indications are calculated with phase detector (PD) along with surpassed via loop filter (LF) to produce fault signal driving voltage-controlled oscillator (VCO) that produces output signal [35][36].

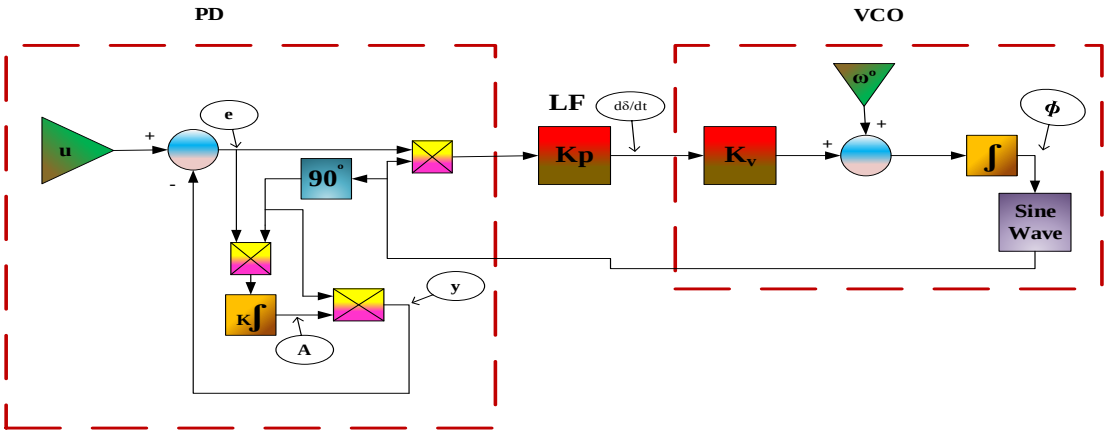

Figure (16) Structure of PLL

In most electrical systems, especially those contain synchronization and PLL techniques, thestage and frequency are estimated in a single loop. However, it will have disturbances as: irregular waveform, line dip/loss, voltage imbalance, Frequency dissimilarity and so on. For the PLL system, these disturbances are able to produce probable glitches [37].

Polluted PLL Output

Irregular waveform of the service will create attenuations that pass in PLL loop via the sampled phase voltages V_a , V_b , V_c. While the irregularity usually does not disturb PLL's locking potential, they will generate attenuation in the output of PLL. The process to abolish attenuations is to employ filters; focus the samples of voltage or focus control loop's the error. Conversely, the PLL system intrinsically contains robust filtering merits because of both the integrators in series in the forward path.

Loss of Gain

Due to the magnitude of the utility voltage shows as a gain term in the forward passageway, any plunge or loss in the line voltage causes unbalance control system's gain. This result is reduced by regularizing the utility magnitude's feedback term.

Phase Deviations

Regarding to the supply frequency, the utility grid is usually an extreme sensitive method. The frequency variation of supply will cause the angle error Δθ to rise. Closed-loop of PLL has expectable response to frequency oscillations in the system. The feed forward term can eradicate the tracking error.

For more accuracy, an extra essential term might be employed in the PI regulator to attain similar effect [38].

VSI control strategies

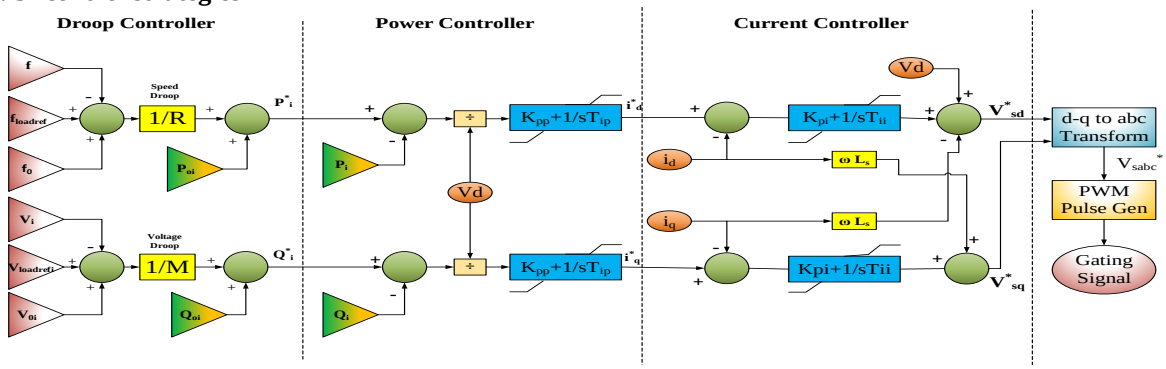

Figure (17) control block drawing in favour of interface inverter gating signal employing control strategies (I. Y. Chung et al. 2010)

Power Control

Power Calculation

Power control measurement can only be initiated when the Operating Mode is Active. This control provides the ability of the controller to sets its output power to a specific value.

To recognize the decoupled vigorous as well spontaneous power controller, 3-Ø current along with voltage of inverter are changed for synchronously revolving reference border (dq) values via Park's transformation, equations of vigorous as well spontaneous power turn out to be:

$$P^{inv} = \frac{3}{2}\left(V_d i_d + V_q i_q\right) \quad (23)$$
$$Q^{inv} = \frac{3}{2}\left(V_q i_q - V_d i_d\right) \quad (24)$$

Once the power control ring produces reference currents depended above equations (3.15) and (3.16), the inner loop is at that time responsible for generating pulses to activate inverter switches, trying to maintain output currents close to reference currents.

droop control

To make MG in reliable operation, it is vital to ensure the shift from grid linked mode to islanding form seen seamless as well keep a stable voltage and frequency regulation throughout islanding mode. Application to make the voltage and frequency within the threshold limit is shown in Figure.18 MG Control Centre (MGCC) can defined locally the reference voltage and frequency values.Phase Locked Loop (PLL) application can measure frequency that is set by [39]:

$$V_{rms} = \sqrt{V_d^2 + V_q^2} \quad (25)$$

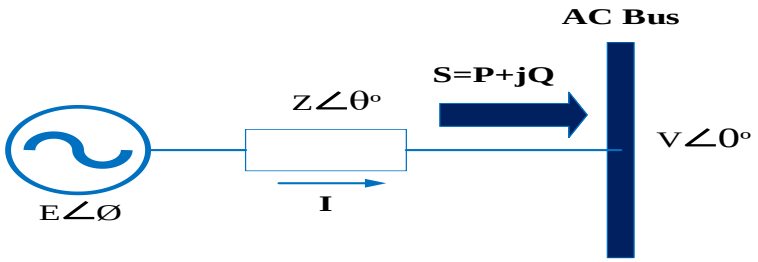

Figure (18) Connection of DG to the AC bus

As microgrid system holds transformers that have important inductance, production energy with rate of recurrence of inverter being guarded depending on reference vigorous as well spontaneous authority of DGs, so Q-V as well P-f droop regulator is generally fine applicants.

$$S = P + jQ \quad (26)$$
$$P = \left(\frac{EV}{Z}cos\emptyset - \frac{V^2}{Z}\right)cos\theta + \frac{EV}{Z}sin\emptyset sin\theta \quad (27)$$
$$P = \left(\frac{EV}{Z}cos\emptyset - \frac{V^2}{Z}\right)sin\theta + \frac{EV}{Z}sin\emptyset cos\theta \quad (28)$$

here, Z, θ, ϕ, E as well V are correspondingly output impedance's enormity, impedance stage position, phase angle dissimilarity among energy of inverter productivity as well PCC, energy enormity of inverter bus as well current of PCC correspondingly. The droop control which used in control strategies in two conventional droop controllers in figure (19).

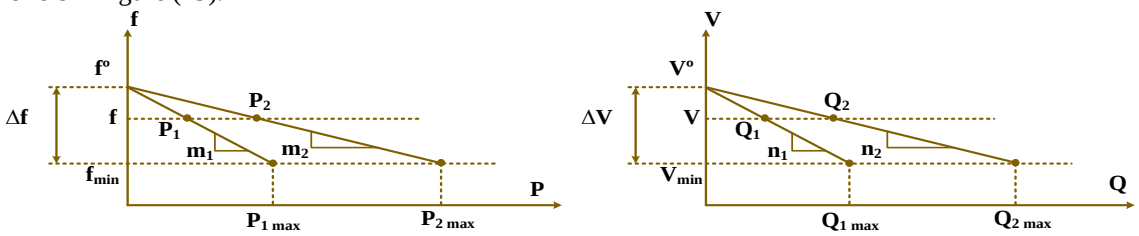

(a) **(b)**

Figure (19) Conventional droop characteristics

$$f = f^* - mP \quad (29)$$
$$V = V^* - nQ \quad (19)$$

where, $V^*$and f^* denotes voltage as well frequency references and E as well ω denotes output voltage along with frequency of the inverter. n as well m denotes frequency and voltage droop coefficients described by Eqs

$$m = \frac{f_{imax} - f_{imin}}{P_{imax} - P_{imin}} \quad (20)$$
$$n = \frac{V_{imax} - V_{imin}}{Q_{imax} - Q_{imin}} \quad (21)$$

n as well as m denotes frequency as well voltage droop coefficients , f_{imax} as well f_{imin} denotes highest as well least rate of frequency in load change, P_{imax}, P_{imin} and Q_{imax}, Q_{imin} denotes highest as well least rates of active as well as reactive power in system respectively. V_{imax} and V_{imin} denotes highest as well least rate of current.

Both droop regulators, rate of recurrence along with voltage-droop regulators, is pertained to load power partaking among generators [40]

$$P^* = P_o + \left(f_o + f_{loadref} - f\right)/m \quad (22)$$

$$Q^* = Q_o + \left(V_o + V_{loadref} - V\right)/n \quad (23)$$

all quantities are given in per unit; P, Q, V, as well f is close by calculated actual as well spontaneous force, bus rms currents along with method rate of recurrence; $f_{loadref}$ and $V_{loadref}$ are load reference indications of rate of recurrence as well current, correspondingly; subscript o signifies fixed rates of regular functioning point for the majority part, f_o as well V_o to be supposed rates, 1.0 p.u. The droop controllers produce references P^* and Q^* by droop qualities.

Voltage and Frequency Controller

The frequency and reference voltage produced from the droop regulator is supplied towards current regulator for forming reference currents at dq reference border. Point of the regulator is for accomplishing preferred estimations of voltage as well frequency through exterminating mistake brought about through DG inclusion else load alterations. This regulator employs two PI controllers whose gain is improved via the proposed metaheuristic method GBO. Numerically, elements of the regulator could be communicated through the equations (24) and (25); regulator directs current as well rate of recurrence dependant on their reference rates (V_{ref} and f_{ref}) along with GBO, clever method that gives optimum manage boundaries for discharging capable reference current vectors. Reference currents is portrayed as [19]

$$i_d^* = \left(v_{ref} - v\right)\left(K_{pv} - \frac{k_{iv}}{s}\right) \quad (30)$$

$$i_q^* = \left(f_{ref} - f\right)\left(K_{Pf} - \frac{k_{if}}{s}\right) \quad (31)$$

Current control strategy

The current controller exercises conservative PI regulators for tracking PWM production current in set points i_d^* as well i_q^*.This regulator or controller is to guarantee that it can accurate following as well short transient of production current. Insulated- gate Bipolar Transistor (IGBT) inverter are applied by six pulses SVPWM. Besides that, to ensure less harmonic distortion in the desired output voltage vectors, SVPWM technique had been used. The voltage signals' reference can be stated [41]:

$$\begin{bmatrix} v_d^* \\ v_q^* \end{bmatrix} = \begin{bmatrix} -k_p & -\omega L_s \\ \omega L_s & -k_p \end{bmatrix} \begin{bmatrix} i_d \\ i_q \end{bmatrix} + \begin{bmatrix} k_p & 0 \\ 0 & k_p \end{bmatrix} \begin{bmatrix} i_d^* \\ i_q^* \end{bmatrix} + \begin{bmatrix} k_i & 0 \\ 0 & k_i \end{bmatrix} \begin{bmatrix} X_d \\ X_q \end{bmatrix} + \begin{bmatrix} V_{sd} \\ V_{sq} \end{bmatrix} \quad (32)$$

With Clarke's transformation, eq. (26) could be changed to a $\alpha\beta$ stationary frame where subsequent equation

$$\begin{bmatrix} v_\alpha \\ v_\beta \\ v_0 \end{bmatrix} = 0.67 \begin{bmatrix} v_a \\ v_b \\ v_c \end{bmatrix} \begin{bmatrix} 1 & -0.5 & -0.5 \\ 0 & 0.87 & -0.87 \\ 0.5 & 0.5 & 0.5 \end{bmatrix} \quad (33)$$

Also, the inductor currents are acquired by Low Pass Filter (LPF). Most of labour, LPF is portrayed as first-order transmit purpose that's exposed,

$$f_l = \frac{1}{1+T_i} f \quad (34)$$

where f is the filter input value, f_l is filtered value, as well T_i is time constant [42].

Use of Virtual Impedance in Inverter Control

It is the idea which used to bring together the temperament of production impedances of inverters running equivalent to one another. The impedance emulates conduct of inductor else resistor in process. Utilizing programmable impedance as opposed to an actual one decreases the misfortunes and cost. Furthermore, being as programmable presents versatile activity as well expands inverter sturdiness beside set of connections impedance deviations [43].

Table (2) Active Reactive Power Droop Controller

Power Control	System Impedance	
	Pure Inductive	Pure Resistance

	$Z_0 = jX_0$	$Z_0 = R_0$
Active Power	$\omega = \omega^* - mP$	$V_{inv} = V^* - nP$
Reactive Power	$V_{inv} = V^* - nQ$	$\omega = \omega^* + mQ$

In Table (2). ω^* and V^* is supposed rate of recurrence as well current of inverter production, m and n, the droop gains, P and Q is standard calculated vigorous as well spontaneous forces, correspondingly.

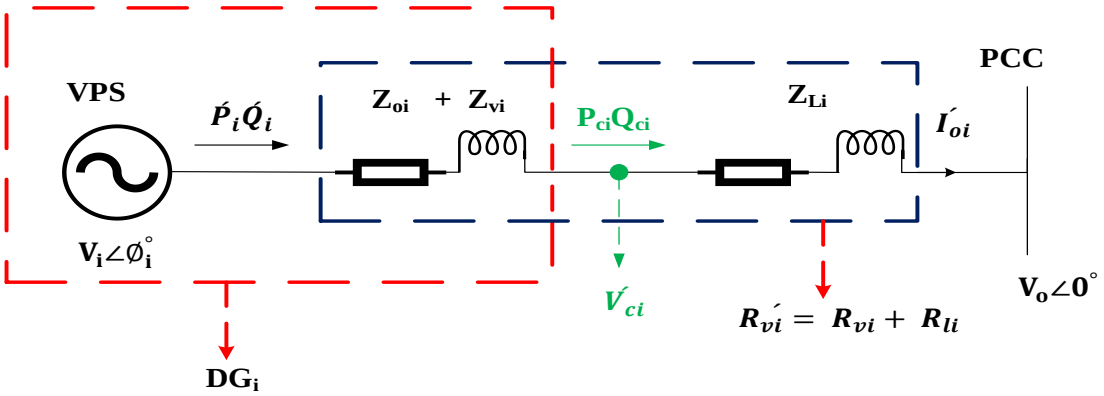

Figure (20) Equivalent circuit of Distributed Generator (DG_i) unit under virtual impedance

From figure (20), the virtual active power $\acute{P}_i$and reactive power$\acute{Q}_i$. The difference between P_{ci} Q_{ci} and $\acute{P}_i\acute{Q}_i$ is the power consumed by $Z_{oi}Z_{vi}$ which may not be negligible.

$$\acute{P}_i = \frac{V_i(V_i - V_o)}{R'_{vi}}\cos(\varphi i) = \frac{V_i(V_i - V_o)}{R'_{vi}} \quad (35)$$

$$\acute{Q}_i = \frac{V_iV_o}{R'_{vi}}\sin(\varphi i) = -\frac{V_iV_o}{R'_{vi}}\varphi i \quad (36)$$

Here φi is believed to be little.

Therefore, the P-V as well Q-ω droop plan could be taken on for normalizing rate of recurrence along with VPS output voltage indication's amplitude.

$$V_i = V^* - m_i\acute{P}_i \quad (37)$$

$$\omega_i = \omega^* - n_i\acute{Q}_i \quad (38)$$

Where m_i and n_i are the droop coefficients. V_i along with ω_i, production current with angular rate of recurrence order [44]. To get an appropriate power contribution among parallel independent DGs, accompanying requirements should be fulfilled:

$$m_{p1}P_1 = m_{p2}P_2 = \cdots = m_{pi}P_{i=}\Delta\omega_{max} \quad (39)$$

$$n_{q1}Q_1 = n_{q2}Q_2 = \cdots = n_{qi}Q_{i=}\Delta V_{max} \quad (40)$$

where $\Delta V_{max}\, and\, \Delta\omega_{max}$ are the allowable boundaries for voltage magnitude and angular frequency deviations, correspondingly [45][46].

CONTROL SYSTEM IN THE DIFFERENT SCENARIOS

Regulation Plan

For assessing suggested regulator plan, the imitation begins in the grid-linked method, consequently microgrid current along with rate of recurrence is generally set up by grid that's accountable for keeping up the profiles.

Moment where microgrid changes towards islanding process sort, The DG unit takes on the V-f power control method dependant on algorithm for relieving voltage fall as well shun rigorous divergence of rate of recurrence brought about through an abrupt shift towards islanding method or load transformation [47][48].

Nonlinear load

Following the exchanging rectifier, fluctuations are evident at this condition. Enormous divergences in reference current totally to DG of bus of nonlinear load is situated is obvious. It adds to low current guideline as production current fall short in following the reference power as to the quick deviations. On behalf of the nonlinear loads it is terminated that major reason for regulator collapses are because of function system of consecutive current along with current regulators. It is intended to be pertained on voltage along with current changeables in dq0 reference border. Within the existence of harmonic deformed loads, time variant (non dc) constituent will be emerged for control changeables. In this way, implanted PI regulators would not pass into making zero stable state fault [49].

Dynamic and steady-state response

To confirm energetic reaction of suggested regulator, a production current of the inverter is moved at many point according to the situation. To begin the stage in the first second with the Microgrid in autonomous mode, another state, the load is changed at specific time. Moreover, when the Microgrid operate in connecting mode. It is visible that the transient time duration is depending on control strategy to reach steady state in these cases. In most control methods, an production filter the inverter is employed move about exchanging harmonics, LPF by small sufficient cut-off rate of recurrence to make sure acceptable reduction for harmonic substance of 'dq' current vectors is employed, to get outcome of waveforms are elevated-class sinusoids through force facto is unison [19][50].

Induction motor in fault condition

The dynamic loads, for example, motor produces significant result at microgrid's presentation. Load dynamics cooperate through ages, also might manipulate steadiness of arrangement [51]. In request to contemplate microgrid's load dynamic through droop control, induction motor as the extensively accepted manufacturing load is selected for analyse. Motor qualities similar to stator as well rotor current along with rotor speed is visible in error situations. The most important reason for unsteadiness is because of great claim of current as well as control[52]. As per the droop feature, DGs rate of recurrence will not succeed for joining as it produce huge quantity for active power as well the age distinction are extraordinary. Reference frequency is verified with power regulators of one of three DGs which are portrayed. To improve the microgrid constancy in three stages to floor error, quick error permission is suggested an answer. If defence method recognizes error as well disengages the piece where small route has occured, method steadiness would be obtained quick [49].

Techniques to scheduling problem and solve power quality issues

For completing control feature principles as well guarantee smooth process for power system throughout and following grid connection, a strong control strategy is fundamentally necessary. Likewise, decrease the dissimilar type of cost of microgrid. Besides, finest limitation of the chosen controller, filters along with additional associated gadgets are obligatory to acquire an ideal vibrant reaction, smooth change, least reconciling time and overshoot. Lately, with the advancement of soft computational techniques, these intentions are successfully accomplished employing different methods of Conventional Strategies and Non-Conventional Strategies [53].Figure() Techniques used in Power quality issues.

Conventional Strategies

In the optimal control system of MG is consist of control loops of power, voltage as well current, by attaining top pace rates of power, voltage and frequency. Proper tune for coefficient of PI controller in outer loop leads to better performance of the system during the fluctuation and load alterations. Many scholars study has been tried to find best strategy of tuning the coefficient of PI controllers in different working cases of MG system. The papers [54][55][56] used "trial and error" method is applied to discover finest values of PI parameters along with giving acceptable performance of the system. However, this method does not assurance the optimal selection of the coefficients and has delay in working time.

Non-Conventional Strategies

These methods employ Artificial intelligence (AI). AI alludes to replication of individual skill in equipments that's modified to believe like public as well copy the actions. The phrase might similarly is related to some mechanism which shows distinctiveness connected through individual psyche like knowledge as well critical opinion. AI methods in microgrid strategies contain Reasoning and Learning (RL) Methods also Swarm Intelligence(SI) methods. RL consist of Fuzzy rule-Based (FB) and Artificial Neuro-Fuzzy Inference System (ANFIS) methods, FB such as Fuzzy logic (FL) method [57][58].

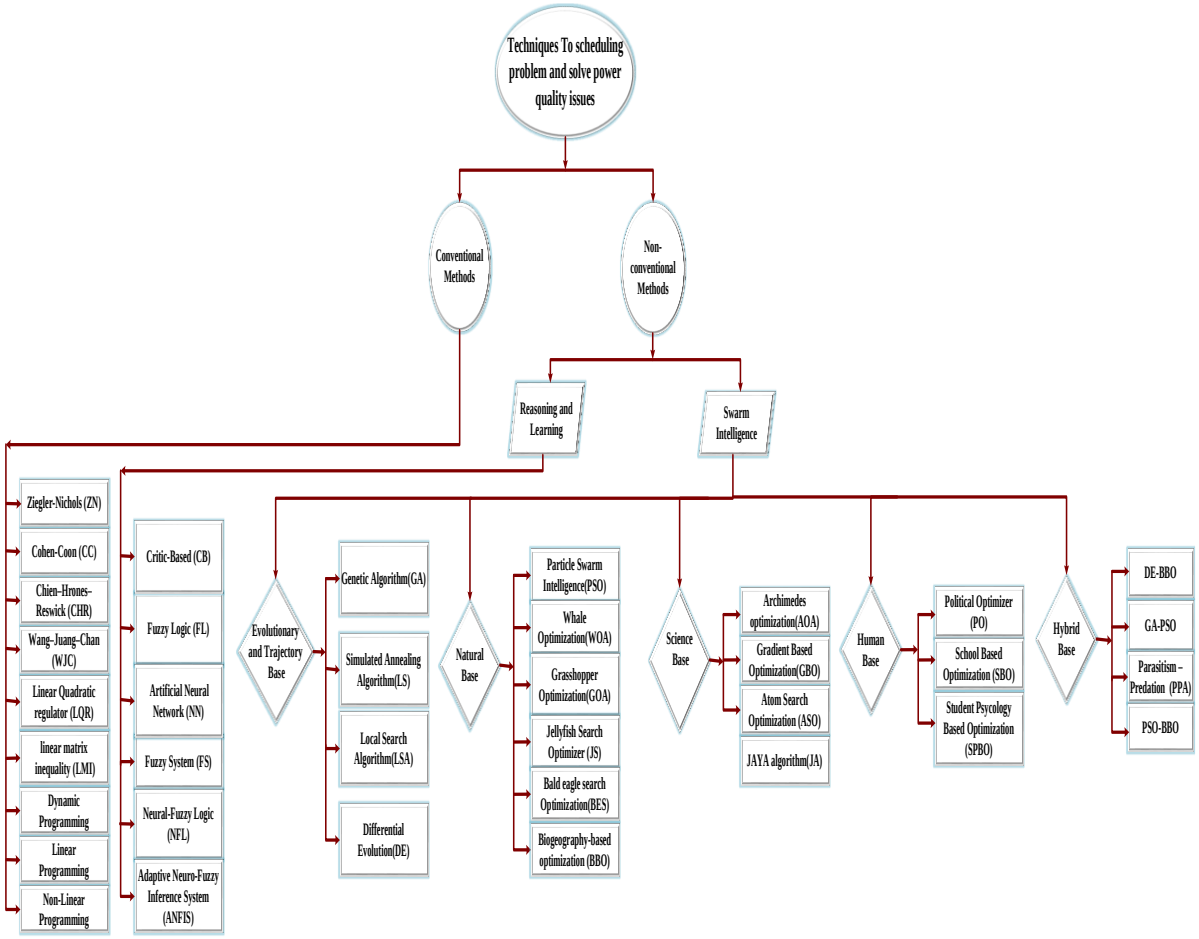

Figure (21) Techniques used in Power quality issues

1.18 Objective function

Particular criterion is given design solution for attaining the system's finest solution using minimization or the maximization and also called target function. These intentional purposes are depended on user inclinations, geological region, tools fixed in microgrid, capability of microgrid, regime policy, kinds of tax, energy storeroom and generation [59]. Generally, in microgrid control strategies, the objective could be single or multiple.

- Single- ojective purpose: there is just a single norm to be advanced, an optimization issue.

- Multi-objective objective: there are few norms to be advanced concurrently[60].

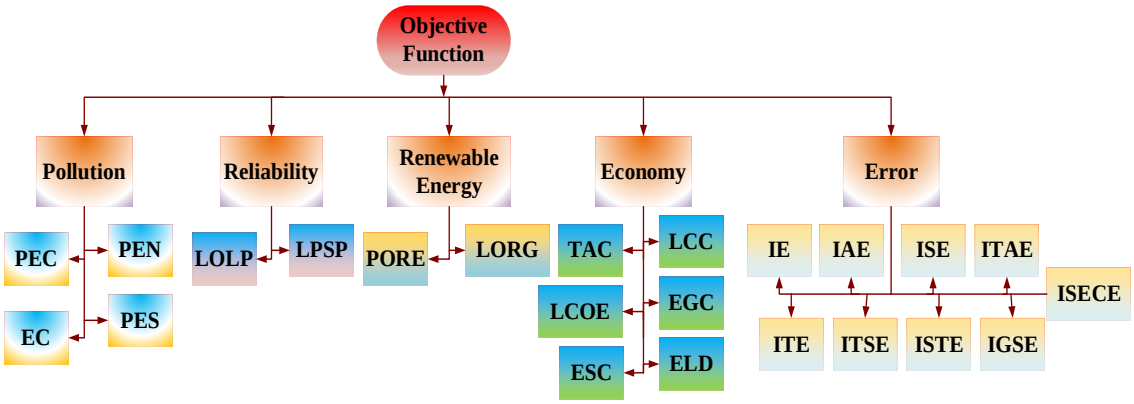

Figure (22) key objective function for the MG optimum operation[61].

In Figure (22) explain different kinds of objective functions used with algorithms. Where Pollution Emission of Carbon Dioxide ⟦CO⟧_2 (PEC), Pollution Emission of Nitrogen oxides ⟦NO⟧_α (PEN), Emission Cost(EC), Pollution Emission of Sulfur Dioxide ⟦SO⟧_2 (PES). Loss of Load Probability (LOLP), Loss of Power Supply Probability (LPSP). Lose for Renewable Generation (LORG), Penetration of Renewable Energy (PORE). Total

Annual Cost (TAC), Lowest Levelized Cost of Energy (LCOE), Life Cycle Cost (LCC), Electricity Generation Cost (EGC), Energy Storage Cost (ESC), Economic Load Dispatch (ELD). Integral Error (IE), Integral Absolute Error (IAE), Integral Time Absolute Error (ITAE), Integral Square Error (ISE), Integral Time Error (ITE), Integral Time Square Error (ITSE), Integral Square Time Error (ISTE), Integral of generalized square error (IGSE), Integral of square error and control effort (ISECE).

Constraints

Various constraints can affect energy management of a microgrid. Power generation's constraints are the greatest and the least control production restrictions. Dispersed generator should function inside the frontiers of protected as well financial activity. A wide range of loads, like housing, business along with manufacturing, devour electric power as indicated by their functioning perimeter. These are expenditure or load constraints[59].

Microgrid's scientific limitations comprise electrical energy in transports, feeder flows, rate of recurrence safety perspectives, start-up as well shut down detachment limitations, just like sloping perimeters. With a portion for examinations, that moreover think about responsive loads, constraints identified with response program must be fulfilled [62]. Add another kind of constraints to figure below

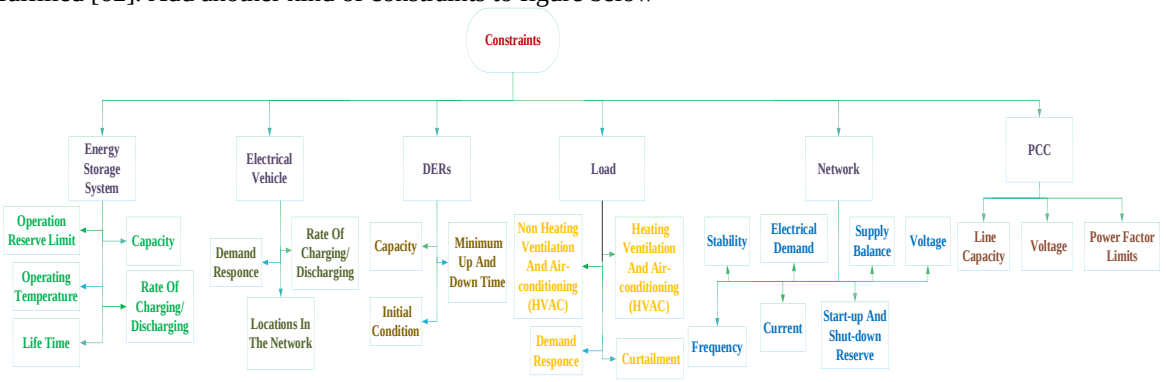

Figure (23) Constraints in The objective Function

1.18.2 Measures of Integral of Error

Measures the control system's performance by calculating integral of controller error. There are many kinds of error functions used as Fitness function such as:

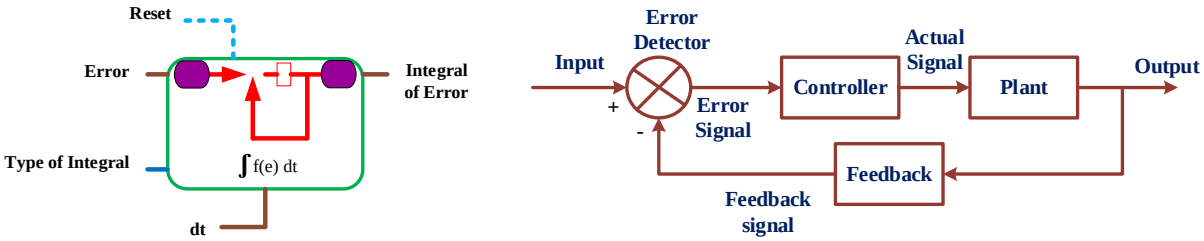

Figure (24) Criterion for calculating the integral of the controller error.

Integral Error (IE) No. (0) Calculates the integral of error using the following equation:

$IE=\int_0^\infty e(t)dt$ (41).

-Integral Absolute Error (IAE) No. (1) Presentation indices as well decrease evaluating great preliminary fault as well as for disciplining minute faults happening afterwards in the reply profoundly. Calculates integral of absolute error using the following equation:

$IAE=\int_0^\infty |e(t)|dt$ (42).

-Integral Square Error (ISE) No. (2) It is the much perceptive means of attaining optimization of integral controller gain. Calculates integral of square error using the following equation:

$ISE=\int_0^\infty [e(t)]^2\,dt$ (43).

-Integral Time Absolute Error (ITAE) No. (3) performance indices as well decrease involvement at big initial fault along with stressing fault shortly in reply. Calculates the integral of time proliferated by total fault using following equation:

$ITAE=\int_0^\infty t\,|e(t)|dt$ (44).

-Integral Time Error (ITE) No. (4) it is only suitable for extremely moist monotonic pace responses of e (t) and easy numerical conduct. Calculates the integral of time multiplied by error using the following equation:

ITE=$\int_0^\infty te\,(t)\,dt$ (45).

-Integral Time Square Error (ITSE) No. (5) performance indices decrease involvement of great early fault and highlight fault later in response. Calculates the integral of time multiplied by square error using the following equation:

ITSE= $\int_0^\infty t\,[e(t)]^2\,dt$ (46).

-Integral Square Time Error (ISTE) No. (6) This performance measure and its generalization are frequently used in linear optimal control and estimation theory. Calculates the integral of square time multiplied by error using the following equation:

ISTE=$\int_0^\infty t^2 e(t) dt$ (47).

-Integral of generalized square error (IGSE) No. (7): It gives better results from ISE are obtained, however, the selection of the weighting factor α is subjective. Calculates the Integral of generalized square error using the following equation.

IGSE=$\int_0^\infty [e^2(t) + \alpha \dot{e}^2(t)]\,dt$ (48)

-Integral of square error and control effort (ISECE) No. (8): Provides a slightly larger emax , but tε becomes essentially smaller as for ; however, the selection of β is subjective. Calculates the Integral of square error and control effort using the following equation.

ISECE= $\int_0^\infty [e^2(t) + \beta u^2(t)]\,dt$ (49)

-benefits of creating minor overruns as well as motions than IAE (integral of the absolute error) or ISE (integral square error) execution indices [63][64][65]. Likewise, that's largely receptive of three, for example, that contains finest choice. ITSE (integral time-square error) lists are fairly fewer responsive and isn't secure computationally [15], [16]. Since it isn't workable to amalgamate for perpetuity, principle is for choosing a rate T adequately great so that e(t) for t > T is unimportant [66].

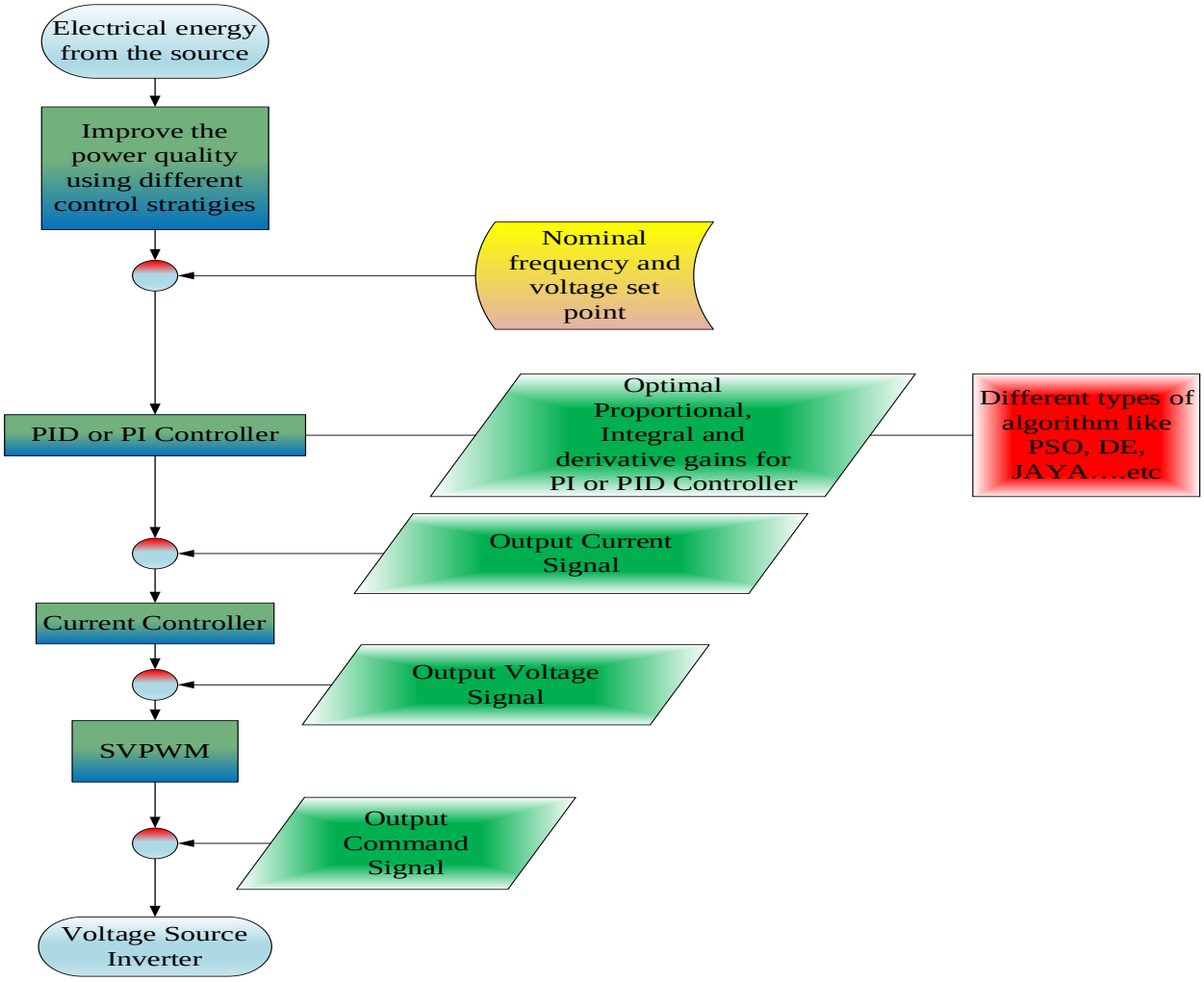

Figure (25). Flow figure of control system for electrical energy supply inverter using different algorithms with different fitness functions [67].

1.18.3 Review on the Use Of Fitness Function

There are many scholars used different strategies to obtain the optimal parameters of PID controllers. Tables(2),(3),(4) and (5) explain these strategies.

Table: 2 Microgrid Operating Modes and Conventional Control Strategies

Ref.	**Mode/Function**	**Description**	**Sources**	**Method**	**Controller**	**Finding**
[55]	Autonomous	VSC, LPF, PWM, Loads	DG1 and DG2	Trial and error method is used.	PI	The performance meet varies in power request, sustain angle/voltage stability and, enhance voltage excellence during the grid-connected and the autonomous

						micro-grid modes of operation
[56]	Both grid connected and islanded modes	2 VSI, 2 PWM, Motor and 2 Sensors	DG1 and DG2	Trial and error method is used.	PI	Voltage and frequency regulation of the microgrid in islanded mode- supply high quality power to its critical loads when a low voltage disturbance occurs in the main network
[68]	(ITSE) and Ziegler Nichols method	Battery, flywheel and aqua-electrolyzer as energy storage elements	WT, PV, diesel generator and FC as power generating sources	Mathematical Test, trial and error method	PID	create that the active responses of the frequency and power of the microgrid is relatively adequate tackle different types of disturbances
[69]	ZN method – LQR and LIM method tune PID	LC filter- VSI- NLL- Induction motor	DC source	linear quadratic regulator (LQR) and linear matrix inequality (LMI)	PID	Acceptable strength and delivers zero steady-state error and rapid transient response. The strength and optimum enactment of the controller is attained –
[51]	Islanded-	VSI- LC filter- PWM – Passive Load-	DC source	ZN- CC- WJC	PID	Fast transient response is achieved, robust

						performance and zero steady-state error in the occurrence of active loads, un-modeled loads, harmonic loads and nonlinear loads.
[70]	LC filter- VSI- Non-linear loads- Induction motor- linear time invariant (LTI)	linear quadratic regulator (LQR) and linear matrix inequality (LMI) as a base for the design of robust PID	DC source	LQR-LMI	PID	The LMI-based PID controller allows almost hundred times better performance as related to the scheme of PID controller utilizing ZN system.

Table 3: Microgrid Operating Modes and Reasoning and Learning Strategies

Ref.	**Mode/Function**	**Description**	**Sources**	**Method**	**Controller**	**Finding**
[71]	Grid-connected- maximum constant boost control (MCBC) method- PI tuned by ZN- MPPT using Incremental Conductance (INC)	Z source-inverter (ZSI)- PWM	PV	MCBC-ZN	PI-FLC	The system response utilizing FLC is other suitable traditional PI controller in terms of less overextend and fewer settling time. Also, the scheme is more stable quickly and sensitively at the preferred value with less oscillation related with PI controller.
[72]	Grid-interfaced – for comparison used PSO with ITAE	VSI- Filter- transformer- Grid-	DC source	ANFIS tune PI	PI controller	High-quality reactive and active power with sinusoidal current- has incredible enhancement in the response speed,

						oscillations in output powers and robust against parametric uncertainties.

Table 4: Microgrid Operating Modes and Swarm Intelligence Strategies

Ref.	**Mode/Function**	**Description**	**Sources**	**Method**	**Controller**	**Finding**
[73]	Autonomus- to minimize the error Function integrated absolute error (IAE) with THD	Universal Bridge Inverter	DC Sourse 650V	PSO	fractional proportional-resonant controller (FPR)	Reduce total harmonic distortion (THD)-better current and voltage waveform
[74]	Grid-connected, - objective functions to be minimized for the DC link voltage(ITAE)and current controller $minF(x) = C_1 \int_0^{T_{max}} t\|e(t)\|\,dt + C_2 \int_0^{T_{max}} THD_V\,dt$ where e is the error, C_1 and C_2 are are weight coefficients, T_{max} is the maximum time, and THD_V is the THD of output voltage	A boost converter, a DC link, an inverter, and a resistor-inductor (RL) filter and is connected to the utility grid through a voltage source inverter	PV panel	PSO	PI controller	The attention of additional input constraints and the optimization of input constraints were recognized to be the two main factors that subsidize the important improvement in power feature control.- minimizing the error to reduce over- shoot, transient response, and steady-state error- voltage and cur- rent stabilization, harmonics reduction, and frequency stability
[75]	Grid connected- objective function to	Boost converter, a	PV	PSO	PI controller	reduces transient peak injection to

	minimize F where Ripple Factor $RF\% = (V_{dc)max} - V_{dc\_min})/V_{dc\_ref}$ $F = \alpha RF\% + \alpha THD\%$	DC-link, an inverter, a LCL filter and the external grid-MPPT technique known as Perturb & Observe (P&O)				the grid consequently improving the transient dynamics of the complete system
[76]	grid connected-objective function to minimize J_T^i $J_T^i = \sum_{k=1}^{n}\sum_{j=1}^{m}(w_1 J_{\Delta P_{jk}} + w_2 J_{\Delta Q_{jk}})$ $J_{\Delta P_{jk}} = ITSE_{\Delta P}$ $J_{\Delta Q_{jk}} = ITSE_{\Delta Q}$	(PCC) , two-level VSI, A passive low-pass filter (LPF) , power electronic interfaces (PEIs)	PVs	PSO	PI controller	Improved PEI performance indices conclude the effectiveness of this systematic controller self-tuning methodology, ensuring enhanced operation of PEIs under real-time weather conditions, reduction of transient energy
[39]	Connected mode - The objective function is to minimization of error function Integral Time Absolute Error (ITAE)	VSI-SVPWM-PLL-LPF	DG unit(PV) - grid	Particle Swarm Optimization (PSO)	PI	PQ control mode show satisfactory power flow when the load power is larger or significantly lower than the rated power of the DG unit
[47]	Autonomous mode-objective function to	VSI-SVPWM-PLL-LPF	DG unit(PV) - grid	PSO	PI	Excellent response for regulating the

	minimization of error function Integral Time Absolute Error (ITAE)					voltage and frequency, and achieves short transient time with a satisfactory harmonic distortion level.
[77]	Connected- Minimize error function in Integral Square Error (ISE)	PCC-VSI-DC/DC converter-	PV module- Grid	Particle Swarm Optimization (PSO)	PI controller-	Satisfactory power flow is achieved for both the cases that is load requirement is greater or lesser than the power generated from MG unit.
[78]	Autonomous/ minimize square error in inner and outer loop using function of integral squared error (ISE)	two-level voltage source converter (VSC)- series filter- (RLC) load	3 DG units	water cycle algorithm (WCA)	Four PI controllers	Acceptable performance of tracking the reference voltages and has a fast and damped transient response with a short settling time and excellent steady state error

Table 5: Combined Strategies

No	Mode/ function	Description	Sources	Method	controller	finding
[79]	Autonomous- Used ZN- PSO and MANFIS/PSO to tune PID	magnetic flywheel system (MFS)	Fuel Cell	combine MANFIS and PSO	PID	Overcome the characteristic disadvantages and enhance the output concert of the fuel cell stack utilized in an EV. Under

						the dynamic operating conditions, the controller adequately spreads the essential EV system.
[80]	Connected mode/ objective function to minimize error function of power $P_{HRES}(s) = \sum_j P_{WT}(s) + P_{PV}(s) + P_{FC}(s) + P_{Bat}(s)$	The hybrid renewable energy source (HRES) ,(SVPWM)-DC/DC converter-Rectifier-	PV array, wind turbine (WT), fuel cells (FC), and battery-Load	A hybrid squirrel search algorithm (SSA)with whale optimization algorithm(WOA)	PI regulators , (SVPWM)	generates the optimal control signal-Develop An efficient control strategy for optimal power flow management of HRES based on the power variation.-
[81]	islanded minimization of error function Integral Time Absolute Error (ITAE)	Use fuzzy lgic-Improved-salp swarm optimized type-II fuzzy controller in load frequency control of multi area islanded AC microgrid	Diesel Engine Generator, Micro turbine, Fuel Cells, Wind turbine generator, Photo Voltaic, Battery Energy Storage	type-II fuzzy with Improved-salp swarm optimized (ISSO)	PID controller	able to balance the power generation and demand properly and control both system frequency and tie-line power effectively
[82]	Autonomous - Minimize function Integral of Time	Mathematica l and matlab representatio	WT , PV, FC and micro	whale	fuzzy cascade	The system better to regulate

	Absolute Error (ITAE)	n of the system of sources and controllers	sources like diesel engine, battery energy storage and flywheel energy storage	optimization algorithm (WOA)	PD-PI controller	frequency in an islanded AC micro grid system under various parametric regions, and various operating conditions
[28]	Islanded/ minimum overshoot/undershoo t – minimize rise time- minimize sitting(response) time- minimize error function Integral Time Absolute Error (ITAE)	Voltage Source Convertor (VSC)	One DG size: 15 kVA	Hybrid Big Bang-Big Crunch (HBB-BC) algorithm which is evolved from PSO and BB-BC	PI regulator- - Fuzzy logic	handle of multiple rules- optimally control the voltage of a DG inverter - adjusts voltage and frequency of the DG with better power quality
[83]	**Autonomous/ Multi-objective function including voltage overshoot/undersho ot, rise time, settling time, and ITAE**	**Voltage Source Convertor (VSC)**	**One DG size: 15 kVA**	**Pareto-based Big Bang-Big Crunch algorithm which is evolved from PSO and BB-BC and fuzzy logic**	**PI regulator -**	**efficient operation of the system- optimal gains of the voltage controller to optimize the response**

1.18.4 Cost Functions

Cost function related with systems which contain large number of sources and other components. In real world the performance and designing of electric system built on two purposes; one is to sustain the economy and the other is to save the reliability of the system[84][85]. Cost Function in algorithm is one of the major optimization challenges in industrial autonomous power system and gets accumulative importance as the total cost and energy demand is growing globally around the world. The process involves dividing the energy demand of generating power system for online thermal units in such method that their operating cost is best while filling the power demand to the customers and constraints sufficiently[86][87].the figure (26) explain the flow chart of algorithm with cost function and Table(6) discus the use of different cost functions with algorithms

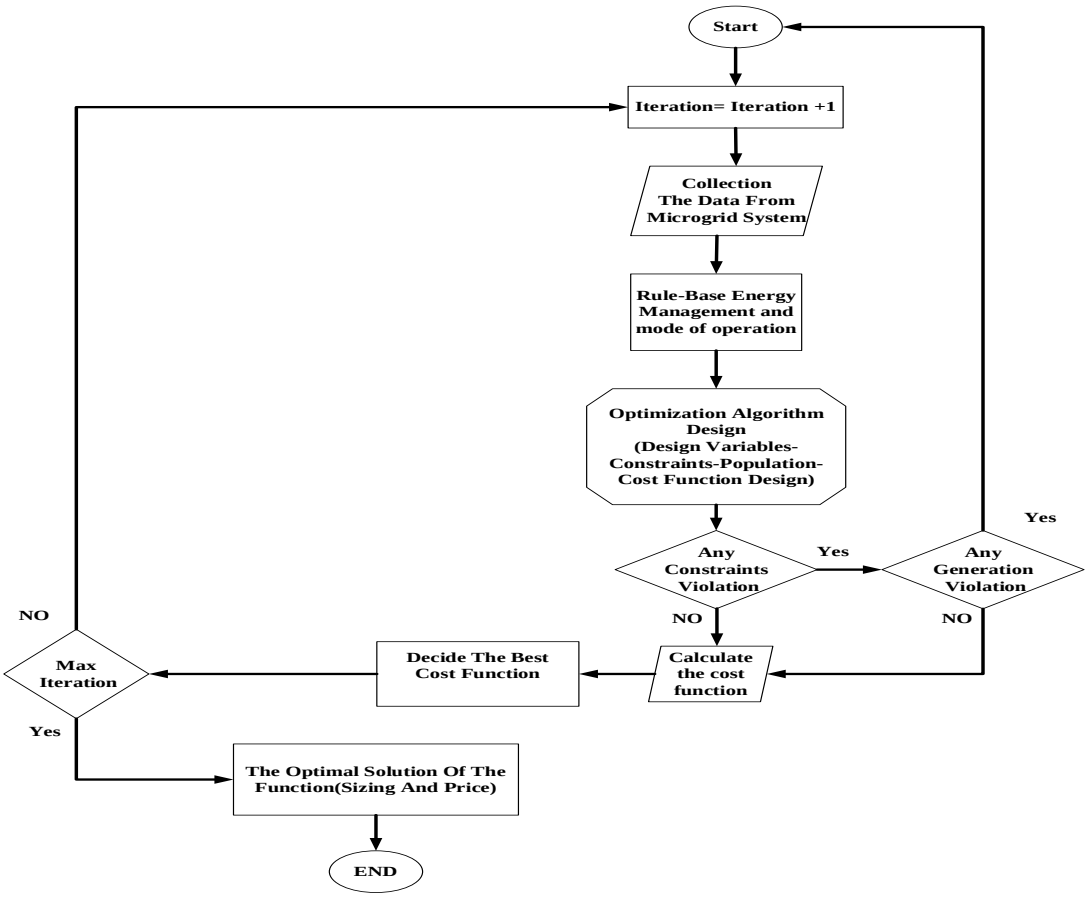

Figure (26) the flow chart of algorithm with cost function

1.18.5 Review on the utilize of cost function

There are many researchers utilize different cost functions to obtain the optimal location and sizing microgrid components. Table (6) explain these functions.

Table(6)the use of different cost functions with algorithms

Ref.	Algorithm, Function Name and Explain	Equation
[88]; [89]	Ant-Lion Optimizer algorithm(ALO) ; regrouping particle swarm optimization (RegPSO) Production Cost (PC) consist of: $F_i(P_i(t))$ is fuel cost function for a diesel generator. SC_i(t) is the initial price function at time t, $C_{OM,i}(t)$ is the running and servicing price of Distributed Generation(DG) at time (t), $C_{OMwind}(t)$ is the running and servicing price cost of the wind generation system at time t, $P_{wind}(t)$ is the predicted wind power at time t, C_{OMpv} is the running and servicing cost of the PV units at time t, $P_{pv}(t)$is the predicted PV generation at time t, $C_{OMes,j}(t)$ is the running and servicing cost of the j th power storage system at time t, $P_{es,j}(t)$ is the j th power storage charging/discharging at time t.	$$Min \sum_{t=1}^{n} \left\{ \begin{array}{l} \sum_{i=1}^{m} (F_i(P_i(t)).T_i(t) + SC_i(t)) + \\ \sum_{i=1}^{m} C_{OM,i}(t)P_i(t) + C_{OMwind}(t)P_{wind}(t) + \\ C_{OMpv}(t)P_{pv}(t) + \sum_{i=1}^{m} C_{OMes,j}(t)P_{es,j}(t) + \end{array} \right\}$$ Where n is the number of time steps, m is the number of all types of DGs,

[90]	genetic algorithm(GA) Total Operation Cost(TOC) consist of: $\sum_{i=1}^{NG}(F(p_i)X_{i,t} + SU_{i,t} + SD_{i,t})$ is power output price, $\sum_{t=1}^{T}\lambda_t P_t^{PCC}$ is represent the start running price. $\sum_{j=1}^{J} La_j\, C_j^L \lambda_j$ is switch off running price. $\sum_{t=1}^{T}\sum_{s=1}^{S} N_{s,t}^{SW}\,\lambda^{sw}$ is represents the buying fees of energy from the upstream network. $F(p_i)X_{i,t}$ is the fuel cost consuming formula. λ_t is a price of buying power at the t th time period. λ^{sw} is the cost of each switching action. $N_{s,t}^{SW}$ is the turn on and turn off actions of the s th switchs at the t th time period.	$$Min\sum_{t=1}^{T}\left\{\begin{array}{l}\sum_{i=1}^{NG}(F(p_i)X_{i,t} + SU_{i,t} + SD_{i,t}) + \\ \sum_{t=1}^{T}\lambda_t P_t^{PCC} + \\ \sum_{j=1}^{J} La_j\, C_j^L \lambda_j + \\ \sum_{t=1}^{T}\sum_{s=1}^{S} N_{s,t}^{SW}\,\lambda^{sw}\end{array}\right\}$$
[91]	artificial bee colony (ABC) algorithm Levelized cost of energy (LCOE)contains: Annualized System Cost (ASC), Total useful energy served(TUES).Where C_{sol} , C_{batt} , C_{wind} and C_{inv} are the cost of solar PV panel, battery, wind turbine and inverter individually. . The term C_x represent the cost of any component where (C) and the component type(x) which could be solar PV panel, battery, wind turbine or inverter. (C_x) has numerous parts such as: installation and Capital cost (C_x^{acap}), replacement cost (C_x^{arep}), annual maintenance cost (C_x^m), operation cost (C_x^f) and salvage cost (C_x^{sal}). The factor called recovery factor (CRF) is used to calculate the cost of each component annually which is utilized to calculate recent value of money.	$LCOE = \frac{ASC(\$/year)}{TUES(KWh/year)}$ $Minimize: ASC = F(N_{sol}C_{sol} + N_{wt}C_{wind} + N_{batt}C_{batt} + P_{inv}C_{inv} + P_{bmg}C_{bmg})$ $C_x = C_x^{acap} + C_x^{arep} + C_x^m + C_x^f + C_x^{sal}$ $CRF(i,N) = \frac{i(1+i)^N}{(1+i)^N - 1}$ (54)
[92]	moth-flame optimization algorithm(MFOA) Net Present Cost(NPC) is used to compute the whole-life cost of the micro-grid. where RC, CC and $O\&M$ characterise replacement, the capital, and maintenance and operation costs, correspondingly; where CRF and K indicate the capital recovery and single payment existing worth factors, individually. Where N is the optimal size of every component, ir indicates the real interest rate, R is the suggested total project lifetime (years), and L characterises each component's lifetime (years).	$NPC = N \times (CC + RC \times K + O\&M \times \frac{1}{CRF(ir,R)} - SV)$(54) $CRF(ir,R) = \frac{ir(1+ir)^R}{(1+ir)^R - 1}$ $K = \sum_{P=1}^{Y}\frac{1}{(1+ir)^{L\times P}}$ $Y = \begin{cases}\left(\left\lceil\frac{R}{L}\right\rceil - 1\right) & if\ \ R\ is\ dividable\ to\ L \\ \left(\left\lceil\frac{R}{L}\right\rceil\right) & if\ \ R\ is\ not\ dividable\ to\ L\end{cases}$ $SV = \mathrm{RC} \times \frac{L_{rem}}{L}$ $L_{rem} = L - (R - L_{rep})$ $L_{rep} = \mathrm{L} \times \left\lceil\frac{R}{L}\right\rceil$

	SV represent the recover value for modules having smaller lifetime than the project, so after replacement the lifetime of these components is extended. L_{rem} represents the remaining life time of each component at the end project lifetime. L_{rep} denotes the replacement cost duration. Where NPC_{PV} , NPC_{WT} , NPC_{bat} , NPC_{inv} , and NPC_{EVSE} address the $NPCs$ of the PV boards, WTs, Battery paks, inverter, and the EVSE, separately. pen_{load} and pen_{lot} are two punishment factors that are used to change over the previously mentioned unwavering quality files to limited costs when the considered dependability limitations are not met (note the single-target definition of the issue). pen_{bat} is a punishment factor used to fuse the constaint on SOC State Of Charge of the battery bank toward the finish of operational time frameinto the ideal estimating technique by adding a boundless expense to the complete NPC of the microgrid in the cases that it has not been fulfilled	$NPC_{total} = NPC_{PV} + NPC_{WT} + NPC_{bat} + NPC_{inv} + NPC_{EVSE} + pen_{load} + pen_{lot} + pen_{bat}$
[93]	improved ant colony optimization(IACO)algorithm Annual system cost (C_{total}) and loss Power Supply Probability (LPSP). Where devices price (DEC), energy waste price (EWC) and hydrogen profit price (HPC). C_{INV} represents speculation price, $C_{O\&M}$ denotes running and servicing price, C_{REP} addresses the substitution price and T_{Sys} the lifespan of the total network. where C_{PV}, C_{WG}, C_{Bat}, C_{EL}, C_{FC}, C_{HY} and C_{INV} are the price of the PV, wind turbine, battery, electrolyzer, FC, hydrogen tank and inverter, separately. N_{PV}, N_{WG}, and N_{HY} are the quantity of the PV, wind turbine, and hydrogen tank, respectively. α is a coefficient. where i is the ratio of profit and T_{Bat}, T_{EL} and T_{FC} are the lifespan of the battery, electrolyzer and FC, respectively.	$C_{total} = C_{DEC} + C_{EWC} - C_{HPC}$ $C_{DEC} = (C_{INV} + C_{O\&M} + C_{REP})/T_{Sys}$ $C_{INV} = C_{PV} \times N_{PV} + C_{WG} \times N_{WG} + C_{Bat} + C_{EL} + C_{FC} + C_{HY} \times N_{HY} + C_{INV}$ $C_{O\&M} = \alpha \times C_{INV} \times T_{Sys}$ $C_{REP} = C_{Bat} \times N_{Bat} \times \sum_{n}^{\frac{T_{Sys}}{T_{Bat}}} \frac{1}{(1+i)^{n \times T_{Bat}}} + C_{EL} \times N_{EL} \times \sum_{n}^{\frac{T_{Sys}}{T_{EL}}} \frac{1}{(1+i)^{n \times T_{EL}}} + C_{FC} \times N_{FC} \times \sum_{n}^{\frac{T_{Sys}}{T_{FC}}} \frac{1}{(1+i)^{n \times T_{FC}}}$ $C_{EWC} = \sum \frac{C_{DEC}}{E_{out-annual}} \times (P_{gen}(t) - P_L(t) - P_{stor}(t))$ $C_{HPC} = \sum \frac{C_{DEC}}{E_{out-annual}} \times \frac{E_{HY}(i)}{\eta_{el}}$ $LPSP = \frac{\sum Time(if\ P_{avai}(t)) < P_L(t))}{T}$

	C_{EWC} represent Energy Waste price. $E_{out-annual}$ denotes the energy generated by the unit yearly. $P_{gen}(t)$, $P_L(t)$ and $P_{stor}(t)$ are the energy created, burned-through and put away at time t, separately. C_{HPC} addresses hydrogen benefit price. where $E_{HY}(i)$ is the energy in hydrogen storage toward the finish of each season and η_{el} is the electrolyzer proficiency. T represent the quantity of hours in the test period and $P_{avai}(t)$ is the existing Power.	$P_{avai}(t) = P_{PV}(t) + P_{WT}(t) + P_{Bat}(t) + P_{HY}(t)$
[94], [95], [96]	Firefly Algorithm (FA); Hybrid chaotic search, harmony search and simulated annealing (CS-HS-SA) algorithm; simulated annealing (SA) algorithm Electricity Generation Cost (EGC). where LCC signifies the lifespan price, CRF is the Investment recovery factor and $E_{Load}(t)$ is load profit at the time(t). where C_{init} denotes the primary price of the network units (including fee of structure work, establishment and interconnections), and C_{main} and C_{rep} are servicing and substitution prices respectively. These two fees are repeat all through the life long of the system. $P_{wor\ fact}$ certainty addresses the current worth factor of the price if the part would be bought n years after the beginning of the project. C_{acq} is the purchase price of the part. i addresses the rate of inflation which is ratio of the lifespan drop in the estimation of cash. r is the ratio of price reduction annually; n addresses the number of years from now until the end life of the project. C_{main} indicates The total price of servicing. where C_{m0} is the servicing price in the starting year. This fee is stated as a portion of the part's price. the network reliability is stated as expression of Load Dissatisfaction Rate (LDR). where $E_{Load}(t)$ is the necessary energy at hour t, T is the interval examination of the network, and $E_{supp}(t)$ is the hourly power supplied to the end-users.	$EGC = \frac{LCC \times CRF}{\sum_{t=1}^{8760} E_{Load}(t)}$ $LCC = C_{init} + C_{main} + C_{rep}$ $C_{rep} = P_{wor\ fact} \times C_{acq}$ $P_{wor\ fact} = \left[\frac{1+i}{1+r}\right]^n = X^n$ $X = \left[\frac{1+i}{1+r}\right]$ $C_{main} = (C_{m0}) \times \left[\frac{1+X^n}{1+X}\right] \times (X)$ $LDR = \frac{\sum_{t=1}^{T}(E_{Load}(t) - E_{supp}(t))}{\sum_{t=1}^{T} E_{Load}}$ (%) $E_{supp}(t) = [E_{Prod}(t) + E_{Bat}(t-1) - E_{Bat,Min}]\eta_{inv}$ $E_{Bat\ Char}(t) = E_{Bat}(t-1) + [E_{Prod}(t) - \frac{E_{Load}(t)}{\eta_{inv}}] \times \eta_{Bat}$ $E_{Bat\ DisChar}(t) = E_{Bat}(t-1) - [\frac{E_{Load}(t)}{\eta_{inv}} - E_{Prod}(t)]$

	where $E_{Bat\ Char}(t), E_{Bat\ DisChar}(t)$ and $E_{Bat}(t-1)$ are the energy in battery bank(per W h) during charge and discharge modes at hour t and $t-1$, $E_{Prod}(t)$ is the total energy created by PV and wind turbine units; $E_{Load}(t)$ is load required at the time t; η_{inv} and η_{Bat} are the effectiveness of inverter and charge effectiveness of battery bank, respectively.	
[97]	Total annual price (TAC) and Loss of Power Supply Probability (LPSP) Where, Investment recovery factor (CRF), C represent unit price of wind turbine, Photovoltaic panel, battery, and converter/inverter.While, N represent number of wind turbine, PV panel, battery, and converter/inverter. where i is the ratio of profit and n represent the whole life time of the system. Some components of PV/WT/batteries/ $Conv\ or\ Inv$ require for substitution many times during the system life span, so (s) represent the replacement time of the component. C_x represent is the present worth cost where C is the price and x is present worth of components PV/WT/batteries/ $Conv\ or\ Inv$ need. where $C_{PV,M}$ and $C_{WT,M}$ are the yearly servicing price of PV and wind turbine. The servicing price of battery and converter/inverter units are ignored. Where LPS is the loss of power supply when the generated energy, E_{Gen}, is less than the load required energy.	$\text{TAC} = \text{Capital Cost} + \text{Maintenance Cost}$ $Capital\ Cost = CRF \times [N_{WT} \times C_{WT} + N_{PV} \times C_{PV} + N_{Battery} \times C_{Battery} + N_{Conv\ or\ Inv} \times C_{Conv\ or\ Inv}]$ $CRF = \frac{i(1+i)^n}{(1+i)^n - 1}$ $C_x = P_x \times P_{wor\ fact}$ $P_{wor\ fact} = \left(1 + \frac{1}{(1+i)^s} + \frac{1}{(1+i)^{2s}} + \cdots + \frac{1}{(1+i)^{n-s}}\right)$ $\text{Maintenance Cost} = N_{PV} \times C_{PV,M} + N_{WT} \times C_{WT,M}$ $LPSP = \frac{\sum_{t=1}^{T} LPS(t)}{\sum_{t=1}^{T} E_{Load}(t)}$ $LPS(t) = E_{Load}(t) - E_{Gen}(t)$
[98]	harmony search (HS)algorithm Total Annual Cost (TAC) TAC comprises of the yearly capital worth (C_{cpt}), the yearly upkeep cost (C_{Mtn}), and the absolute yearly expense of fuel utilization of the diesel generator (C_{Fuel}) with ($). capital recuperation factor (CRF). where i is the loan fee and n signifies the life expectancy of the framework.	$TAC = C_{cpt} + C_{Mtn} + C_{Fuel}$ $CRF = \frac{i(1+i)^n}{(1+i)^n - 1}$ $C_{FC/Elect} = (P_{FC/Elect} + P^{ins}_{FC/Elect}) \times P_{wor\ fact}$ $P_{wor\ fact} = \left(1 + \frac{1}{(1+i)^s} + \frac{1}{(1+i)^{2s}} + \cdots + \frac{1}{(1+i)^{n-s}}\right)$ $C_x = P_x \times P_{wor\ fact}$ For example $C_{Conv/Inv} = P_{Conv/Inv} \times P_{wor\ fact}$

	where $C_{FC/Elect}$ is the current cost of FC/electrolyzer framework, $P_{FC/Elect}$ is FC/electrolyzer cost and $P_{FC/Elect}^{ins}$ indicates FC/electrolyzer establishment worth. A few parts of PV/WG/diesel/FC networks should be substituted a few times over the task life time (n). The substitution of part is (s). where $C_{Conv/Inv}$ is the current worth of converter/inverter parts and $P_{Conv/Inv}$ is the converter/inverter cost. C denote unit cost of wind turbine, PV board, battery, Fuel Cell, diesel generator and converter/inverter.While, N address number of wind turbine, PV board, battery, Fuel Cell, diesel generator and converter/inverter.	$C_{cpt} = CRF \times [N_{WT} \times C_{WT} + N_{PV} \times C_{PV} + N_{Battery} \times C_{Battery} + N_{FC/Elect} \times C_{FC/Elect} + N_{Conv\ or\ Inv} \times C_{Conv\ or\ Inv} + N_{Diesel} \times C_{Diesel}]$ $C_{Mtn} = N_{PV} \times C_{Mtn}^{PV} + N_{WT} \times C_{Mtn}^{WT} + C_{Mtn}^{FC} + C_{Mtn}^{Elect} + C_{Mtn}^{Diesel}$
[99]	crow search algorithm(CSA) Economic load dispatch (ELD), Valve point loading effect (VPE), Emission dispatch (ED), Combined economic–emission dispatch (CE-ED) Where, Cost Function of Conventional generation (CFC), fossil-fueled generators (FFG) where P is the generation output of the DER. u_g, v_g and w_g are the price factors of the gth non-sustainable units. C_{RES}; C_{ESS} and C_{grid} are the price factors of RES, ESS and utility grid cost, respectively. $F(P_{DER})$ is in \$/h. target Function of non-sustainable generating units with Valve point stacking effect(CFC-VPE) Where δ and θ are the VPE coefficients of the gth unit. The emanation dispatch formula ($E(P_{FFG})$) The unit of $E(P)$ is kg/h. where x_g, y_g and z_g are the emission parameters of the gth unit. combined economic–emission dispatch (CEED) where h_g is the punishment factor of the gth unit. The unit of h_g is \$/kg. The price of sustainable generating units (C_{RES}) where G^E is the running and servicing price of the RES utilized. C_{DC} represent the consumption price of the DGs which is with kilowatt hour. The peak generation power of the DG described by (P_{max}), the hourly output generation of the DG denoted by (P_r). While the peak	$F(P_{DER}) = CFC\ of\ FFG + C_{RES} * (P_{RES}^t) + C_{ESS} * (P_{EES}^t) + C_{grid} * (P_{grid}^t)$ $CFC - FFG = \sum_{t=1}^{24} \sum_{b=1}^{ESS} \sum_{r=1}^{RES} \sum_{g=1}^{FFG} \{u_g * (P_g^t)^2 + v_g * (P_g^t) + w_g\}$ $CFC - VPE = \sum_{t=1}^{24} \sum_{g=1}^{FFG} \{u_g * (P_g^t)^2 + v_g * (P_g^t) + w_g + |\delta_g sin\theta_g (P_{g,min}^t - P_g^t)|\}$ $E(P_{FFG}) = \sum_{t=1}^{24} \sum_{g=1}^{FFG} \{x_g * (P_g^t)^2 + y_g * (P_g^t) + z_g$ $CEED = \sum_{t=1}^{24} \sum_{g=1}^{FFG} [\{u_g * (P_g^t)^2 + v_g * (P_g^t) + w_g\} + h_g * \{x_g * (P_g^t)^2 + y_g * (P_g^t) + z_g\}]$ $C_{RES} = C_{DC} + G^E$ $C_{DC} = \frac{DC}{P_r^{max} \times 8760 \times cf} \times P_r$ $DC = IC \times \frac{k(1+k)^l}{(1+k)^l - 1}$

	power in hour depicted by (P_r^{max}) and its ability factor is (cf) . Establishment price is denoted by (IC), ratio of profit represented by 'k' and the life cycle time of the DG units described by 'l'.	
[100]	gravitational search algorithm(GSA) Energy Production Cost(EPC) where m is the number of time intervals in the plane time horizon T. $C_t^g, C_t^{\acute{g}}$ describe the fee of power generated by sustainable and non-sustainable units in t interval. C_t^{ES+}, C_t^{ES-} present the price of energy supplied by ES units during charging and releasing running modes in $t\ interval$. C_t^l is the fee of energy expended by reacting load required (RLD) and Ω_t is the punishment fee coming from because of undelivered energy (UP) among the time span t. where $\pi_t^{k.g}, \pi_t^{'k.g}$ address the offer costs by the k th sustainable and non-sustainable units during t interval, $P_t^{k,g}, P_t^{'k,g}$ are generation of k th sustainable and non-sustainable resources during t interval, n^g, n'^g show the quantity of sustainable and non-sustainable resources connected in the MG network, Δt is length of t interval, $\pi_t^{k.l}$ is related to offer cost by the k th RLD during t interval, $P_t^{k,l}$ is expanded generation by the k th RLD during t interval, π_t^{UP} is the offer cost when the network has UP. P_t^{UP} is the quantity of powerin MG that has not been delivered.	$$EPC = min \sum_{t=1}^{m} \left(C_t^g + C_t^{'g} + C_t^{ES-} - C_t^l - C_t^{ES+} + \Omega_t\right) \times \Delta t$$ $$C_t^g = \sum_{k=1}^{n^g} (\pi_t^{k.g} \times P_t^{k,g})$$ $$C_t^{'g} = \sum_{k=1}^{n'^g} (\pi_t^{'k.g} \times P_t^{'k,g})$$ $$C_t^l = \sum_{k=1}^{n^l} (\pi_t^{k.l} \times P_t^{k,l})$$ $$C_t^{ES+} = \sum_{k=1}^{n^{ES}} (\pi_t^{k.ES+} \times X_t^{ES} \times P_t^{k,ES+})$$ $$C_t^{ES-} = \sum_{k=1}^{n^{ES}} (\pi_t^{k.ES-} \times (1 - X_t^{ES}) \times P_t^{k,ES-})$$ $$\Omega_t = (\pi_t^{UP} \times P_t^{UP})$$
[101]	multi-objective self-adaptive multi-population based Jaya(MO-SAMP-JA) algorithm Electricity Price Cost(EPC) and Pollution Emission of Carbon Dioxide CO_2 (PEC) Where δ addresses time interval, The output generation of PV unit (S_t), solar cell's effectiveness is denoted by η^{PV} . μ^E and r are the servicing fee of ESS and PV separately. b_t is the electrical energy cost at time t, G_t the stored energy and $G_t^{sell,Grd}$ the power bought from the	$$EPC = min \sum_t \left[\delta(rS_t/\eta^{PV} + b_t\left(G_t - G_t^{sell,Grd}\right) + \mu^E B_t)\right]$$ $$S_t = \eta^{PV}\ AR^{PV} R_t (1 - 0.005(TEM - 25))$$ $$E_t = E_{t-1} + \eta\delta A_t - \delta B_t/\eta$$ Or $EPC = min\ \sum_t \left[\delta(rS_t/\eta^{PV} + b_t\left(G_t - G_t^{sell,Grd}\right) + \mu^E B_t + p\gamma_t)\right]$ Or $EPC = min\ \sum_t \left[\delta(rS_t/\eta^{PV} + b_t\left(G_t - G_t^{sell,Grd}\right) + \mu^E B_t)\right] + qG^{max}$ $$PEC = \sum_t \delta \xi_t^G G_t$$

	upstream network. while B_t is the energy acquired from the ESS . A_t denotes the energy provided to the ESS. AR^{PV} is size of photovoltaic board. Sun insolation is signified as R_t. TEM represent the temperature of the surrounding. p is the disparity between high and standard power required cost from the upstream network. $w1$ and $w2$ are the factors appointed to the target function EPC and PEC respectively. That changes over the multi-target function into single target function and thereafter find the best optima of the function.	$Multi\ objective\ function = \min\ (w1 \times EPC + w2 \times PEC)$
[102]	integer value and the power from the grid utility a continuous value INTLINPROG solver for mixed integer linear programming (MILP) total life cycle cost (TLCC) Where: p is the quantity of parts to be bought identified with the venture, I_{nvst} means the capital cost, $C_{O\&M}$ indicates running & servicing cost, C_{repl} signifies the substitution cost, C_{salv} is the rescue cost, C_f is the price of energy per kWh, t_s is the testing interval, $P_{grid}(t)$ means network generation. A_{PV} represent the size of solar panels, $I(t)$ means the insulation of Solar system occurrence on the solar panels at time t, η_{PV} indicates the proficiency of the solar system, R_B is the mathematical operator that addresses the rate of the insolation incident on solar panel to the standard insolation on horizontal solar panel , $I_B(t)$ is the hourly general insolation in the area and $I_D(t)$ is the diffuse insolation, η_r signifies the efficiency of so the module ranked by the industry, η_{Pc} is the generation effectiveness, β is the proficiency temperature operator of the generator, limited between 0.004 and 0.006 C∘, T_c temperature of the panel. $NOCT$ means the typical working cell temperature. An average estimation of $NOCT$ equivalents to 45 C∘, $P_{grid}(t)$ means the	$TLCC = \min\left(w\sum_{q=1}^{p}\left(I_{nvst}(q) + C_{O\&M}(q) + C_{repl}(q) - C_{salv}(q)\right) + (1-w)C_f\sum_{t=7}^{18} t_s P_{grid}(t)\right)$ $P_{PV}(t) = \eta_{PV} A_{PV} I(t)$ $I(t) = R_B(I_B(t) + I_D(t)) + I_D(t)$ $\eta_{PV} = \eta_r \eta_{Pc}(1 - \beta(T_c - NOCT))$ $T_c = 30 + 0.0175(I(t) - 300) + 1.14(T_c - 25)$ $E_{grid} = \sum_{t=7}^{18} t_s P_{grid}(t)$ $COE = C_f \sum_{t=7}^{18} t_s P_{grid}(t)$ $P_{inv}(t) = P_{PV}(t)\,\eta_{inv}$ $LCC = I_{nvst} + C_{O\&M} + C_{repl} - C_{salv}$ $\begin{cases} O\&M = (O\&M)_o \times \frac{1+f}{1-f}\left(1 - \left(\frac{1+f}{1-f}\right)^N\right), i \neq f \\ O\&M = (O\&M)_o \times N,\ \ i = f \end{cases}$ $I_{invst} = IC_{PV} + IC_{inv}$ $IC_{PV} = 1.2 X_{PV} C_{PV} \sum_{t=7}^{18} P_{PV}(t)$ $IC_{inv} = 1.2 Pr_{inv} C_{inv} = 1.2 X_{PV} K_{inv} C_{inv} \sum_{t=7}^{18} P_{PV}(t)$ $TLCC = LCC_{PV} + LCC_{inv}$ $LPSP = \frac{\sum_{t=7}^{18} LPS(t)}{\sum_{t=7}^{18} P_L(t)}$ $LPS(t) = P_{inv}(t) + P_{grid}(t) - P_L(t)$

generation of network, and t_s is the testing time, E_{grid} and COE are The energy and the price of it which bought from the fundamental lattice between 7:00h and18:00h respectively, $P_{inv}(t)$ The generation of the inverter, and η_{inv} signifies proficiency of inverter.

IC_{PV} represents the primary fee of solar system, and IC_{inv} signifies the primary fee of inverter, X_{PV} means the number of solar boards, C_{PV} addresses investment price of solar array per KW, and $P_{PV}(t)$ means the generation of the solar system at time t, C_{inv} means the investment price of inverter per kW, Pr_{inv} generation ratio of inverter, K_{inv} the outsized factor of inverter, X_{PV} indicates the quantity of photovoltaic boards, LCC_{PV} signifies the lifespan price of solar boards, and LCC_{inv} means the lifespan price of inverter.

$LPS(t)$ denotes loss of generation supply at the testing time (t), while $P_L(t)$ is the hourly end user power need. Loss of force supply likelihood $LPSP$ is supposed to be in the range of 0 and 1.

$multi\ target\ function$

The initial term addresses the complete life span price of the project, and second term addresses power bought from the stream network. w means the gauging operator chose to figure out the overall significance of bringing down each term in every target function. i represents the degree of profit, t_s the testing interval, and Pr_{PV} indicates the generation ratio of solar cells.

$$multi\ target\ function = \min\left(w\left[C_{PV}\left(1.2 + 0.1 \times \frac{1+f}{1-f}\left(1 - \left[\frac{1+f}{1+i}\right]^{N}\right)\right) + 2.2\eta_{inv}K_{inv}C_{inv}\sum_{t=7}^{18} t_s X_{PV} P_{PV}(t) Pr_{PV}\right] + (1-w)C_f \sum_{t=7}^{18} t_s P_{grid}(t)\right)$$

1.19 Termination Criteria

While meta heuristic algorithm is utilized for sorting out optimization crisis, cessation criterion ought to be put to carry greatest number of iterations or the recurring deciphering method to stop. A few investigations obtain greatest period span for procedure into account, as well as erstwhile classify a satisfactory fault among two successive principles of price utility [45]. The final optimal solution, the cost function ought to give ideal estimating of system component or best load subsequent act, uphold power, electrical energy as well as rate of recurrence at microgrid close to supposed principles in addition to carefully maintain it inside cutoff points[46][103] .

1.20 Conclusion

MGs are chief segments of a fresh epoch of current age. The frameworks proved their capacity for managing force stream productivity in addition to moderation for decrease of glasshouse gases. Other than DC generations

contain simple arrangement in addition to current improved proficiency on AC systems, elevated housing as well as manufacturing utilization requires VSI; the plans play out specific exercises to oversee electrical energy on MG.

The managing arrangement of VSI is upgraded in energy-cost idea to necessitate minimization of an intention purpose beneath imperatives. Considering an expansive guideline plot because of potential clashes between its variables. Besides, it searches for worldwide manage of a scheme beating contentions of goals as well as convalescing execution. It is important to recognize efficient estimating and activity strategies to lessen the expense of the power. Furthermore, because of natural issues, we are compelled to look for plan which utilizes flammable basis all the more effectively. Besides, MGs is shown as an incredible innovation which builds urban areas as well as networks much upholding as well as flexible. Various sorts of price utility that are utilized in MG optimization are existing.

Future fashions illustrate the potential lines of investigation in the part. Elevated communications of goals in MGs have directed to novel as well as inventive recommendations for accomplishing improved control, organization and management of the system.

References

1. Z. A. Arfeen et al., "Insights and trends of optimal voltage-frequency control DG-based inverter for autonomous microgrid: State-of-the-art review," Int. Trans. Electr. Energy Syst., vol. 30, no. 10, pp. 1–26, 2020, doi: 10.1002/2050-7038.12555.

2. H. Akagi and A. Nabae, "The p-q theory in three-phase systems under non-sinusoidal conditions," in European Transactions on Electrical Power, 1993, vol. 3, no. 1, pp. 27–31, doi: 10.1002/etep.4450030106.

3. W. J. L. Ferrero A., Morando A. P., Ottoboni R., Superti-Furga G., "On the Meaning of the Park Power Components in Three-Phase Systems under Non-Sinusoidal Conditions," J. Stat. Mech. Theory Exp., vol. 3, no. 1, pp. 33–43, 1993, doi: 10.1088/1742-5468/2010/03/L03005.

4. S. S. Mitra, Madhuchhanda, Surajit Chattopadhyay, "Chapter 12 Clarke and Park Transform," in Electric Power Quality (Power Systems), Springer Netherlands, 2011, pp. 89–96.

5. Ø. Grøn, "Chapter 15 SPACE GEOMETRY IN ROTATING REFERENCE FRAMES :," in Relativity in Rotating Frames, Springer, 2004, pp. 285–333.

6. B. W. Franca, L. F. Da Silva, and M. Aredes, "Comparison between alpha-beta and DQ-PI controller applied to IUPQC operation," COBEP 2011 - 11th Brazilian Power Electron. Conf., pp. 306–311, 2011, doi: 10.1109/COBEP.2011.6085231.

7. M. Castilla, J. Miret, A. Camacho, J. Matas, and L. G. De Vicuna, "Reduction of current harmonic distortion in three-phase grid-connected photovoltaic inverters via resonant current control," IEEE Trans. Ind. Electron., vol. 60, no. 4, pp. 1464–1472, 2013, doi: 10.1109/TIE.2011.2167734.

8. T. A. Jumani, M. W. Mustafa, M. M. Rasid, N. H. Mirjat, M. H. Baloch, and S. Salisu, "Optimal power flow controller for grid-connected microgrids using grasshopper optimization algorithm," Electron., vol. 8, no. 1, 2019, doi: 10.3390/electronics8010111.

9. X. Wang, F. Blaabjerg, and Z. Chen, "Autonomous control of inverter-interfaced distributed generation units for harmonic current filtering and resonance damping in an islanded microgrid," IEEE Trans. Ind. Appl., vol. 50, no. 1, pp. 452–461, 2014, doi: 10.1109/TIA.2013.2268734.

10. X. Wang, F. Blaabjerg, and Z. Chen, "An improved design of virtual output impedance loop for droop-controlled parallel three-phase voltage source inverters," 2012 IEEE Energy Convers. Congr. Expo. ECCE 2012, pp. 2466–2473, 2012, doi: 10.1109/ECCE.2012.6342404.

11. Z. Ke et al., "VSG Control Strategy Incorporating Voltage Inertia and Virtual Impedance for Microgrids," Energies, vol. 13, no. 16, p. 4263, 2020, doi: 10.3390/en13164263.

12. P. Dattaray, D. Chakravorty, P. Wall, J. Yu, and V. Terzija, "A Novel Control Strategy for Subsynchronous Resonance Mitigation Using 11 kV VFD-Based Auxiliary Power Plant Loads," IEEE Trans. Power Deliv., vol. 33, no. 2, pp. 728–740, 2018, doi: 10.1109/TPWRD.2017.2711624.

13. H. Elmetwaly, A. A. Eldesouky, and A. A. Sallam, "An Adaptive D-FACTS for Power Quality Enhancement in an Isolated Microgrid," IEEE Access, vol. 8, pp. 57923–57942, 2020, doi: 10.1109/ACCESS.2020.2981444.

14. Ren, X. Sun, S. Chen, and H. Liu, "A compensation control scheme of voltage unbalance using a combined three-phase inverter in an Islanded microgrid," Energies, vol. 11, no. 9, 2018, doi: 10.3390/en11092486.

15. M. H. Andishgar, M. Gholipour, and R. allah Hooshmand, "Improved secondary control for optimal unbalance compensation in islanded microgrids with parallel DGs," Int. J. Electr. Power Energy Syst., vol. 116, no. September 2019, p. 105535, 2020, doi: 10.1016/j.ijepes.2019.105535.

16. Y. Jia, D. Li, and Z. Chen, "Unbalanced power sharing for islanded droop-controlled microgrids," J. Power Electron., vol. 19, no. 1, pp. 234–243, 2019, doi: 10.6113/JPE.2019.19.1.234.

17. Vechiu, G. Gurguiatu, and E. Rosu, "Advanced active power conditioner to improve power quality in microgrids," 2010 9th Int. Power Energy Conf. IPEC 2010, pp. 728–733, 2010, doi: 10.1109/IPECON.2010.5697021.

18. C. Natesan, S. K. Ajithan, P. Palani, and P. Kandhasamy, "Survey on Microgrid: Power Quality Improvement Techniques," ISRN Renew. Energy, vol. 2014, no. 16 March 2014, pp. 1–7, 2014, doi: 10.1155/2014/342019.

19. L. R. Srinivas and B. M. Ram, "Voltage and Frequency control of Distribution Differential Evolution .," in International Conference on Intelligent Computing and Control Systems (ICICCS), 2018, vol. 2, pp. 772–778.

20. J. D. Bastidas-Rodríguez, C. A. Ramos-Paja, J. David Bastidas-Rodríguez, and C. Ramos-Paja, "Types of inverters and topologies for microgrid applications Tipos," UIS Ing., vol. 16, no. 1, pp. 7–14, 2017.

21. C. H. C. and D. S. H. Jae Hyeong Seo, "A New Simplified Space – Vector PWM Method for Three-Level Inverters," IEEE Trans. Power Electron., vol. 16, no. 4, pp. 545–550, 2001, doi: 10.1109/APEC.1999.749730.

22. N. Patil, J. Celaya, D. Das, K. Goebel, and M. Pecht, "Precursor parameter identification for insulated gate bipolar transistor (IGBT) prognostics," IEEE Trans. Reliab., vol. 58, no. 2, pp. 271–276, 2009, doi: 10.1109/TR.2009.2020134.

23. V. K. Khanna, Insulated gate bipolar transistor IGBT theory and design. John Wiley & Sons, 2004.

24. J. W. Sheen, "A Compact Semi-Lumped Low-Pass Filter for Harmonics and Spurious Suppression," IEEE Microw. Guid. Wave Lett., vol. 10, no. 3, pp. 92–93, 2000, doi: 10.1109/75.845707.

25. S. E. B. Sabri, M. Z. Bin Sujod, and M. S. Bin Jadin, "Comparative study on the performances of PV system with various combinations of converter topologies and PWM types," J. Telecommun. Electron. Comput. Eng., vol. 10, no. 1–2, pp. 25–29, 2018.

26. U. Tahir et al., "Design of three phase solid state transformer deployed within multi-stage power switching converters," Appl. Sci., vol. 9, no. 17, 2019, doi: 10.3390/app9173545.

27. Iqbal, A. Lamine, I. Ashraf, and Mohibullah, "MATLAB/SIMULINK model of space vector PWM for three-phase voltage source inverter," 41st Int. Univ. Power Eng. Conf. UPEC 2006, Conf. Procedings, vol. 3, no. 2, pp. 1096–1100, 2006, doi: 10.1109/UPEC.2006.367646.

28. M. Sedighizadeh, M. Esmaili, and A. Eisapour-Moarref, "Voltage and frequency regulation in autonomous microgrids using Hybrid Big Bang-Big Crunch algorithm," Appl. Soft Comput. J., vol. 52, pp. 176–189, 2017, doi: 10.1016/j.asoc.2016.12.031.

29. G. C. and Y. L. Kiam Heong Ang, "PID Control System Analysis, Design and Technology," Ambient. Bentônico, Vol 3, vol. 13, no. November, pp. 559–576, 2005, doi: 10.1016/b978-85-352-7263-5.50018-7.

30. T. A. Jumani et al., "Jaya optimization algorithm for transient response and stability enhancement of a fractional-order PID based automatic voltage regulator system," Alexandria Eng. J., vol. 59, no. 4, pp. 2429–2440, Aug. 2020, doi: 10.1016/j.aej.2020.03.005.

31. M. S. Mahmoud, N. M. Alyazidi, and M. I. Abouheaf, "Adaptive intelligent techniques for microgrid control systems: A survey," Int. J. Electr. Power Energy Syst., vol. 90, no. 3 March 2017, pp. 292–305, 2017, doi: 10.1016/j.ijepes.2017.02.008.

32. E. Çam and I. Kocaarslan, "Load frequency control in two area power systems using fuzzy logic controller," Energy Convers. Manag., vol. 46, no. 2, pp. 233–243, 2005, doi: 10.1016/j.enconman.2004.02.022.

33. M. Tali, A. Esadki, T. Nasser, and B. Boukezata, "Active power filter for power quality in grid connected PV-system using an improved fuzzy logic control MPPT," Proc. 2018 6th Int. Renew. Sustain. Energy Conf. IRSEC 2018, 2018, doi: 10.1109/IRSEC.2018.8703018.

34. C. C. Lee, "Fuzzy Logic in Control Systems: Fuzzy Logic Controller, Part I," IEEE Trans. Syst. Man Cybern., vol. 20, no. 2, pp. 404–418, 1990, doi: 10.1109/21.52552.

35. M. K.-G. and M. R. Iravani, "A New Phase-Locked Loop (PLL) System," in Proceedings of the 44th IEEE 2001 Midwest Symposium on Circuits and Systems. MWSCAS 2001 (Cat. No. 01CH37257), 2001, pp. 421–424.

36. J. C. H. Hsieh, Guan-Chyun, "Phase-locked loop techniques. A survey," in IEEE Transactions on industrial electronic, 1996, pp. 609–615.

37. M. Karimi Ghartemani, S. A. Khajehoddin, P. K. Jain, and A. Bakhshai, "Problems of startup and phase jumps in PLL systems," IEEE Trans. Power Electron., vol. 27, no. 4, pp. 1830–1838, 2012, doi: 10.1109/TPEL.2011.2169089.

38. V. K. VikramBlasko, "Operation of a phase locked loop system under distorted utility conditions," in IEEE Transactions on Industry applications, 1997, vol. 33, no. 1, pp. 58–63.

39. W. Al-saedi, S. W. Lachowicz, D. Habibi, and O. Bass, "Power flow control in grid-connected microgrid operation using Particle Swarm Optimization under variable load conditions," Int. J. Electr. Power Energy Syst., vol. 49, no. 1, pp. 76–85, 2013, doi: 10.1016/j.ijepes.2012.12.017.

40. Chung, W. Liu, D. A. Cartes, S. Member, and K. Schoder, "Control parameter optimization for a microgrid system using particle swarm optimization," in IEEE International Conference on Sustainable Energy Technologies, 2008, pp. 837–842.

41. W. Al-saedi, S. W. Lachowicz, D. Habibi, and O. Bass, "Electrical Power and Energy Systems Power quality enhancement in autonomous microgrid operation using Particle Swarm Optimization," Int. J. Electr. Power Energy Syst., vol. 42, no. 1, pp. 139–149, 2012, doi: 10.1016/j.ijepes.2012.04.007.

42. K. Sureshkumar and V. Ponnusamy, "Power flow management in micro grid through renewable energy sources using a hybrid modified dragonfly algorithm with bat search algorithm," Energy, vol. 181, pp. 1166–1178, 2019, doi: 10.1016/j.energy.2019.06.029.

43. W. Issa and A. Elkhateb, "Virtual Impedance Impact on Inverter Control Topologies," in 7th International Conference on Renewable Energy Research and Applications (ICRERA), 2018, pp. 1423–1428.

44. Y. L. Chen, Jianbo, Dong Yue, Chun-Xia Dou, Lei Chen, Shengxuan Weng, "A Virtual Complex Impedance based P − V Droop Method for Parallel-connected Inverters in Low-voltage AC

Microgrids," in IEEE Transactions on Industrial Informatics, 2020, pp. 1–10, doi: 10.1109/TII.2020.2997054.

45. M. A. Ebrahim, "Optimal PI Based Secondary Control for Autonomous Micro-grid via Particle Swarm Optimization Technique," pp. 1148–1155, 2018.

46. J. Preetha Roselyn, A. Ravi, D. Devaraj, R. Venkatesan, M. Sadees, and K. Vijayakumar, "Intelligent coordinated control for improved voltage and frequency regulation with smooth switchover operation in LV microgrid," Sustain. Energy, Grids Networks, vol. 22, p. 100356, 2020, doi: 10.1016/j.segan.2020.100356.

47. W. Al-Saedi, S. W. Lachowicz, D. Habibi, and O. Bass, "Voltage and frequency regulation based DG unit in an autonomous microgrid operation using Particle Swarm Optimization," Int. J. Electr. Power Energy Syst., vol. 53, no. 1, pp. 742–751, 2013, doi: 10.1016/j.ijepes.2013.06.002.

48. T. A. Jumani, M. W. Mustafa, A. S. Alghamdi, M. M. Rasid, A. Alamgir, and A. B. Awan, "Swarm Intelligence-Based Optimization Techniques for Dynamic Response and Power Quality Enhancement of AC Microgrids: A Comprehensive Review," IEEE Access, vol. 8, pp. 75986–76001, 2020, doi: 10.1109/ACCESS.2020.2989133.

49. Khaledian and M. Aliakbar Golkar, "Analysis of droop control method in an autonomous microgrid," J. Appl. Res. Technol., vol. 15, no. 4, pp. 371–377, 2017, doi: 10.1016/j.jart.2017.03.004.

50. T. A. Jumani, M. W. Mustafa, M. M. Rasid, N. H. Mirjat, Z. H. Leghari, and M. Salman Saeed, "Optimal voltage and frequency control of an islanded microgrid using grasshopper optimization algorithm," Energies, vol. 11, no. 11, 2018, doi: 10.3390/en11113191.

51. S. K. Sarkar, F. R. Badal, and S. K. Das, "A comparative study of high performance robust PID controller for grid voltage control of islanded microgrid," Int. J. Dyn. Control, vol. 6, no. 3, pp. 1207–1217, Sep. 2018, doi: 10.1007/s40435-017-0364-0.

52. F. R. Badal, P. Das, S. K. Sarker, and S. K. Das, "A survey on control issues in renewable energy integration and microgrid," Prot. Control Mod. Power Syst., vol. 4, no. 1, 2019, doi: 10.1186/s41601-019-0122-8.

53. M. Bajaj and A. K. Singh, "Grid integrated renewable DG systems: A review of power quality challenges and state-of-the-art mitigation techniques," Int. J. Energy Res., vol. 44, no. 1, pp. 26–69, 2020, doi: 10.1002/er.4847.

54. N. Pogaku, M. Prodanović, and T. C. Green, "Modeling, analysis and testing of autonomous operation of an inverter-based microgrid," IEEE Trans. Power Electron., vol. 22, no. 2, pp. 613–625, Mar. 2007, doi: 10.1109/TPEL.2006.890003.

55. F. Katiraei, M. R. Iravani, and P. W. Lehn, "Small-signal dynamic model of a micro-grid including conventional and electronically interfaced distributed resources," IET Gener. Transm. Distrib., vol. 1, no. 3, p. 369, 2007, doi: 10.1049/iet-gtd:20045207.

56. C. K. Sao and P. W. Lehn, "Control and power management of converter fed microgrids," IEEE Trans. Power Syst., vol. 23, no. 3, pp. 1088–1098, 2008, doi: 10.1109/TPWRS.2008.922232.

57. Z. A. Arfeen, M. P. Abdullah, M. F. Shehzad, S. Altbawi, M. A. Khan Jiskani, and M. A. Imran YiRan, "A niche particle swarm optimization- Perks and perspectives," 2020 IEEE 10th Int. Conf. Syst. Eng. Technol. ICSET 2020 - Proc., no. November, pp. 102–107, 2020, doi: 10.1109/ICSET51301.2020.9265384.

58. Z. A. Arfeen et al., "A comprehensive review of modern trends in optimization techniques applied to hybrid microgrid systems," Concurr. Comput. Pract. Exp., p. e6165, Dec. 2020, doi: 10.1002/cpe.6165.

59. Ahmad Khan, M. Naeem, M. Iqbal, S. Qaisar, and A. Anpalagan, "A compendium of optimization objectives, constraints, tools and algorithms for energy management in microgrids," Renew. Sustain. Energy Rev., vol. 58, pp. 1664–1683, 2016, doi: 10.1016/j.rser.2015.12.259.

60. S. Phommixay, M. L. Doumbia, and D. Lupien St-Pierre, "Review on the cost optimization of microgrids via particle swarm optimization," Int. J. Energy Environ. Eng., vol. 11, no. 1, pp. 73–89, 2020, doi: 10.1007/s40095-019-00332-1.

61. M. A. Hannan, S. Y. Tan, A. Q. Al-Shetwi, K. P. Jern, and R. A. Begum, "Optimized controller for renewable energy sources integration into microgrid: Functions, constraints and suggestions," J. Clean. Prod., vol. 256, p. 120419, 2020, doi: 10.1016/j.jclepro.2020.120419.

62. H. Shayeghi, E. Shahryari, M. Moradzadeh, and P. Siano, "A survey on microgrid energy management considering flexible energy sources," Energies, vol. 12, no. 11, pp. 1–26, 2019, doi: 10.3390/en12112156.

63. H. Unbehauen, "Controller Design in Time Domain," in CONTROL SYSTEMS, ROBOTICS AND AUTOMATION, vol. 2, Encyclopedia of Life Support Systems (EOLSS), 2009, pp. 22–30.

64. K. Jagatheesan and B. Anand, "Dynamic performance of multi-area hydro thermal power systems with integral controller considering various performance indices methods," in INternational Conference On Emerging Trends in Science Engineering and Technology (INCOSET), 2012, pp. 474–478, doi: 10.1109/incoset.2012.6513952.

65. N. E. Ambitiously, "LABVIEW NXG 5.0- MANUAL," 2020. [Online]. Available: http://www.ni.com/documentation/en/labview/latest/analysis-control-node-ref/measures-of-integral-of-error/#. [Accessed: 05-Aug-2020].

66. D. Maiti, A. Acharya, M. Chakraborty, A. Konar, and R. Janarthanan, "Tuning PID and PIλDδ Controllers using the Integral Time Absolute Error Criterion," in 4th International Conference on Information and Automation for Sustainability, 2008, pp. 457–462, doi: 10.1109/ICIAFS.2008.4783932.

67. Y. Teekaraman, R. Kuppusamy, and S. Nikolovski, "Solution for Voltage and Frequency Regulation in Standalone Microgrid using Hybrid Multiobjective Symbiotic Organism Search Algorithm," Energies, vol. 12, no. 14, 2019, doi: 10.3390/en12142812.

68. G. Mallesham, S. Mishra, and A. N. Jha, "Ziegler-Nichols based controller parameters tuning for load frequency control in a microgrid," in Proceedings - 2011 International Conference on Energy, Automation and Signal, ICEAS - 2011, 2011, pp. 335–342, doi: 10.1109/ICEAS.2011.6147128.

69. M. A. Nezhad and H. Bevrani, "Frequency control in an islanded hybrid microgrid using frequency response analysis tools," IET Renew. Power Gener., vol. 12, no. 2, pp. 227–243, 2018, doi: 10.1049/iet-rpg.2017.0227.

70. M. Armin, P. N. Roy, S. K. Sarkar, and S. K. Das, "LMI-Based Robust PID Controller Design for Voltage Control of Islanded Microgrid," Asian J. Control, vol. 20, no. 5, pp. 2014–2025, Sep. 2018, doi: 10.1002/asjc.1710.

71. H. A. Mosalam, R. A. Amer, and G. A. Morsy, "Fuzzy logic control for a grid-connected PV array through Z-source-inverter using maximum constant boost control method," Ain Shams Eng. J., vol. 9, no. 4, pp. 2931–2941, 2018, doi: 10.1016/j.asej.2018.10.001.

72. S. Kakkar, R. K. Ahuja, and T. Maity, "Performance enhancement of grid-interfaced inverter using intelligent controller," Meas. Control (United Kingdom), vol. 53, no. 3–4, pp. 551–563, 2020, doi: 10.1177/0020294019879171.

73. B. Amini, R. Roshanfekr, A. Hajipoor, and S. Y. Mousazadeh Mousavi, "Interface converter control of distributed generation in microgrids using fractional proportional—Resonant

controller," Electr. Power Syst. Res., vol. 194, no. June 2020, p. 107097, 2021, doi: 10.1016/j.epsr.2021.107097.

74. M. F. Roslan, Ia. Q. Al-shetwi, M. A. Hannan, P. J. Ker, and A. W. M. Zuhdi, Particle swarm optimization algorithm-based PI inverter controller for a grid-connected PV system. 2020.

75. S. Fahad, A. J. Mahdi, W. H. Tang, K. Huang, and Y. Liu, "Particle Swarm Optimization Based DC-Link Voltage Control for Two Stage Grid Connected PV Inverter," 2018 Int. Conf. Power Syst. Technol. POWERCON 2018 - Proc., no. 201807100000006, pp. 2233–2241, 2019, doi: 10.1109/POWERCON.2018.8602128.

76. Arzani and G. K. Venayagamoorthy, "Computational approach to enhance performance of photovoltaic system inverters interfaced to utility grids," IET Renew. Power Gener., vol. 12, no. 1, pp. 112–124, 2018, doi: 10.1049/iet-rpg.2016.1044.

77. P. Malathi and M. Saravanan, "Power management in microgrid using PI controller tuned by particle swarm optimization," 2017 Innov. Power Adv. Comput. Technol. i-PACT 2017, vol. 2017-Janua, pp. 1–6, 2017, doi: 10.1109/IPACT.2017.8245007.

78. H. M. Hasanien and M. Matar, "Water cycle algorithm-based optimal control strategy for efficient operation of an autonomous microgrid," IET Gener. Transm. Distrib., vol. 12, no. 21, pp. 5739–5746, 2018, doi: 10.1049/iet-gtd.2018.5715.

79. C. N. Huang and Y. S. Chen, "Design of magnetic flywheel control for performance improvement of fuel cells used in vehicles," Energy, vol. 118, pp. 840–852, 2017, doi: 10.1016/j.energy.2016.10.112.

80. M. Durairasan and D. Balasubramanian, "An efficient control strategy for optimal power flow management from a renewable energy source to a generalized three-phase microgrid system: A hybrid squirrel search algorithm with whale optimization algorithm approach," Trans. Inst. Meas. Control, pp. 1–17, 2020, doi: 10.1177/0142331220901628.

81. P. C. Sahu, S. Mishra, R. C. Prusty, and S. Panda, "Improved -salp swarm optimized type-II fuzzy controller in load frequency control of multi area islanded AC microgrid," Sustain. Energy, Grids Networks, vol. 16, pp. 380–392, 2018, doi: 10.1016/j.segan.2018.10.003.

82. P. C. Sahu, R. C. Prusty, and S. Panda, "Frequency regulation of an electric vehicle-operated micro-grid under WOA-tuned fuzzy cascade controller," Int. J. Ambient Energy, vol. 0, no. 0, pp. 1–12, 2020, doi: 10.1080/01430750.2020.1783358.

83. E. Moarref, M. Sedighizadeh, and M. Esmaili, "Multi-objective voltage and frequency regulation in autonomous microgrids using Pareto-based Big Bang-Big Crunch algorithm," Control Eng. Pract., vol. 55, pp. 56–68, 2016, doi: 10.1016/j.conengprac.2016.06.011.

84. P. Chen, H. C.-I. transactions on power systems, and undefined 1995, "Large-scale economic dispatch by genetic algorithm," ieeexplore.ieee.org.

85. R. K. Swain, N. C. Sahu, and P. K. Hota, "Gravitational Search Algorithm for Optimal Economic Dispatch," Procedia Technol., vol. 6, pp. 411–419, 2012, doi: 10.1016/j.protcy.2012.10.049.

86. R. Poli, "Analysis of the Publications on the Applications of Particle Swarm Optimisation," J. Artif. Evol. Appl., vol. 2008, no. 2, pp. 1–10, 2008, doi: 10.1155/2008/685175.

87. Z. L. Gaing, "Particle swarm optimization to solving the economic dispatch considering the generator constraints," IEEE Trans. Power Syst., vol. 18, no. 3, pp. 1187–1195, 2003, doi: 10.1109/TPWRS.2003.814889.

88. K. Roy, K. K. Mandal, and A. C. Mandal, "Ant-Lion Optimizer algorithm and recurrent neural network for energy management of micro grid connected system," Energy, vol. 167, pp. 402–416, 2019, doi: 10.1016/j.energy.2018.10.153.

89. H. Li, A. T. Eseye, J. Zhang, and D. Zheng, "Optimal energy management for industrial microgrids with high-penetration renewables," Prot. Control Mod. Power Syst., vol. 2, no. 1, pp. 1–14, 2017, doi: 10.1186/s41601-017-0040-6.

90. W. C. Yeh et al., "New genetic algorithm for economic dispatch of stand-alone three-modular microgrid in DongAo Island," Appl. Energy, vol. 263, no. January, 2020, doi: 10.1016/j.apenergy.2020.114508.

91. S. Singh, M. Singh, and S. C. Kaushik, "Feasibility study of an islanded microgrid in rural area consisting of PV, wind, biomass and battery energy storage system," Energy Convers. Manag., vol. 128, pp. 178–190, 2016, doi: 10.1016/j.enconman.2016.09.046.

92. S. Mohseni, A. C. Brent, and D. Burmester, "A demand response-centred approach to the long-term equipment capacity planning of grid-independent micro-grids optimized by the moth-flame optimization algorithm," Energy Convers. Manag., vol. 200, no. October, pp. 105–112, 2019, doi: 10.1016/j.enconman.2019.112105.

93. W. Dong, Y. Li, and J. Xiang, "Optimal sizing of a stand-alone hybrid power system based on battery/hydrogen with an improved ant colony optimization," Energies, vol. 9, no. 10, 2016, doi: 10.3390/en9100785.

94. Kaabeche, S. Diaf, and R. Ibtiouen, "Firefly-inspired algorithm for optimal sizing of renewable hybrid system considering reliability criteria," Sol. Energy, vol. 155, pp. 727–738, 2017, doi: 10.1016/j.solener.2017.06.070.

95. W. Zhang, A. Maleki, M. A. Rosen, and J. Liu, "Sizing a stand-alone solar-wind-hydrogen energy system using weather forecasting and a hybrid search optimization algorithm," Energy Convers. Manag., vol. 180, no. May 2018, pp. 609–621, 2019, doi: 10.1016/j.enconman.2018.08.102.

96. W. Zhang, A. Maleki, M. A. Rosen, and J. Liu, "Optimization with a simulated annealing algorithm of a hybrid system for renewable energy including battery and hydrogen storage," Energy, vol. 163, pp. 191–207, 2018, doi: 10.1016/j.energy.2018.08.112.

97. Maleki and F. Pourfayaz, "Optimal sizing of autonomous hybrid photovoltaic/wind/battery power system with LPSP technology by using evolutionary algorithms," Sol. Energy, vol. 115, pp. 471–483, 2015, doi: 10.1016/j.solener.2015.03.004.

98. Maleki and F. Pourfayaz, "Sizing of stand-alone photovoltaic/wind/diesel system with battery and fuel cell storage devices by harmony search algorithm," J. Energy Storage, vol. 2, pp. 30–42, 2015, doi: 10.1016/j.est.2015.05.006.

99. Dey, B. Bhattacharyya, A. Srivastava, and K. Shivam, "Solving energy management of renewable integrated microgrid systems using crow search algorithm," Soft Comput., vol. 24, no. 14, pp. 10433–10454, 2020, doi: 10.1007/s00500-019-04553-8.

100. M. Marzband, M. Ghadimi, A. Sumper, and J. L. Domínguez-García, "Experimental validation of a real-time energy management system using multi-period gravitational search algorithm for microgrids in islanded mode," Appl. Energy, vol. 128, pp. 164–174, 2014, doi: 10.1016/j.apenergy.2014.04.056.

101. Manzoor et al., "A Priori Multiobjective Self-Adaptive Multi-Population Based Jaya Algorithm to Optimize DERs Operations and Electrical Tasks," IEEE Access, vol. 8, pp. 181163–181175, 2020, doi: 10.1109/access.2020.3028274.

102. K. Ndwali, J. G. Njiri, and E. M. Wanjiru, "Multi-objective optimal sizing of grid connected photovoltaic batteryless system minimizing the total life cycle cost and the grid energy," Renew. Energy, vol. 148, pp. 1256–1265, 2020, doi: 10.1016/j.renene.2019.10.065.

103. L. Abualigah, M. Shehab, M. Alshinwan, and H. Alabool, "Salp swarm algorithm: a comprehensive survey," Neural Comput. Appl., vol. 32, no. 15, pp. 11195–11215, 2020, doi: 10.1007/s00521-019-04629-4.